On scenario construction for stochastic shortest path problems in real road networks

Dongqing Zhang and Stein W. Wallace and Zhaoxia Guo and Yucheng Dong and Michal Kaut

Business School, Sichuan University, Chengdu, China

and

NHH Norwegian School of Economics, Bergen, Norway

and

SINTEF, Trondheim, Norway

in: Transportation Research Part E: Logistics and Transportation Review. See also BibTeX entry below.

BibTeX:

```
@article{ZhangEtAl2021,
  author    = {Dongqing Zhang and Stein W. Wallace and Zhaoxia Guo and Yucheng Dong and Michal Kaut},
  journal   = {Transportation Research Part {E}: {L}ogistics and Transportation Review},
  title     = {On scenario construction for stochastic shortest path problems in real road networks},
  year      = {2021},
  pages     = {102410},
  volume    = {152},
  doi       = {10.1016/j.tre.2021.102410},
  publisher = {Elsevier {BV}}
}
```


The original publication is available at DOI 10.1016/j.tre.2021.102410.

Document created on July 6, 2021.

On scenario construction for stochastic shortest path problems in real road networks

Dongqing Zhang[a], Stein W. Wallace[a,b], Zhaoxia Guo[a,*], Yucheng Dong[a], Michal Kaut[c]

[a] *Business School, Sichuan University, Chengdu, China*
[b] *NHH Norwegian School of Economics, Bergen, Norway*
[c] *SINTEF Technology and Society, Trondheim, Norway*

Abstract

Stochastic shortest path (SSP) computations are often performed under very strict time constraints, so computational efficiency is critical. A major determinant for the CPU time is the number of scenarios used. We demonstrate that by carefully picking the right scenario generation method for finding scenarios, the quality of the computations can be improved substantially over random sampling for a given number of scenarios. We study extensive SSP instances from a freeway network and an urban road network, which involve 10,512 and 37,500 spatially and temporally correlated speed variables, respectively. On the basis of experimental results from a total of 42 origin-destination pairs and 6 typical objective functions for SSP problems, we find that (1) the scenario generation method generates unbiased scenarios and strongly outperforms random sampling in terms of stability (i.e., relative difference and variance) whichever origin-destination pair and objective function is used; (2) to achieve a certain accuracy, the number of scenarios required for scenario generation is much lower than that for random sampling, typically about 6-10 times lower for a stability level of 1% in the freeway network; and (3) different origin-destination pairs and different objective functions could require different numbers of scenarios to achieve a specified stability.

Keywords: Stochastic shortest path; spatial and temporal correlation; scenario generation; random sampling; number of scenarios; stability

1. Introduction

The shortest path problem, with variants such as the quickest path problem, is a classical combinatorial optimization problem, which is to find a path in a

*Corresponding author

Email addresses: dqzhang1123@gmail.com (Dongqing Zhang), stein.wallace@nhh.no (Stein W. Wallace), zx.guo@alumni.polyu.edu.hk (Zhaoxia Guo), ycdong@scu.edu.cn (Yucheng Dong), michal.kaut@sintef.no (Michal Kaut)

network (or graph) from an origin node to a destination node with the shortest link length or quickest travel time. This problem has been the subject of extensive research for many years (Deo and Pang, 1984), due to its diverse applications in routing problems in road networks (Ehmke et al., 2016; Prakash, 2018), packet routing problems (Krioukov et al., 2004) and Internet distance predictions (Shavitt and Tankel, 2008) in Internet networks, distance queries in social networks (Akiba et al., 2013), and disease-disease interactions in biological networks (Maiorino et al., 2020). Most papers deal with deterministic problems, see reviews (Sommer, 2014; Bast et al., 2016) and relevant papers in recent years (Hu and Sotirov, 2019; Brown and Carlyle, 2019).

Real-world shortest path problems are stochastic in nature due to unpredictable factors such as traffic accidents, traffic control and weather conditions in road networks, and unpredictable transmission requests in Internet networks. The stochastic shortest path (SSP) problem attempts to capture the uncertainty associated with the edges by modelling the weights on edges as random variables. Various SSP problems have been investigated in road networks (Ehmke et al., 2016; Prakash, 2018) and in Internet networks (Shavitt and Tankel, 2008). Typical objectives to be optimized in previous SSP studies involve such as the minimization of expected travel time (Prakash, 2018), the minimization of expected carbon emission (Ehmke et al., 2016), the minimization of a linear combination of travel time mean and standard deviation (Zhang et al., 2017), and the minimization of travel time budget for a specified on-time arrival probability (Chen et al., 2018). The majority of previous studies on SSPs assume that travel speeds on different road links and across different time periods are uncorrelated (Miller-Hooks and Mahmassani, 2000; Prakash, 2018; Pedersen et al., 2020). But in recent years, an increasing number of papers consider spatially correlated speeds (Zhang et al., 2017; Prakash and Srinivasan, 2018) in road networks, that is, the speed on one link is correlated with the speeds on certain other links.

It is reasonable to assume that there exists strong spatial and temporal correlation among link travel speeds in real road networks, largely due to traffic flow propagations over time and space, or an event, for example dynamic traffic management (Köster et al., 2018), that affects traffic capacities in a wide area (Rachtan et al., 2013). Guo et al. (2020) have demonstrated that this is indeed the case based on the real speed datasets from an urban road network and a freeway network. Temporal correlation in speeds means that the speed in one time period is correlated with the speed in other time periods. The spatial and temporal correlations have been studied by some researchers (Cheng et al., 2012; Rachtan et al., 2013; Guo et al., 2020), and considered in several travel time- and route-related decision-making problems (Zou et al., 2014; Avraham and Raviv, 2020). The significance of spatial and temporal correlation of stochastic speeds in SSP problems has also been demonstrated by Huang and Gao (2012), Zockaie et al. (2013), and Zockaie et al. (2016). Huang and Gao (2012) and Zockaie et al. (2013) found that spatial and temporal correlations could affect the optimal path and the impact was related to the levels of correlation. Zockaie et al. (2016) discovered that the optimal path travel time distribution in the

spatially and temporally correlated case fell between the uncorrelated case and the spatially correlated case.

However, the SSP research with both spatially and temporally correlated stochastic speeds (or travel times) is still in its infancy, although there are several studies reported in recent years (Huang and Gao, 2012; Zockaie et al., 2013; Yang and Zhou, 2014; Zockaie et al., 2016). Some researchers (Hu et al., 2018; Yang et al., 2018) have presented effective methods for path finding of SSP problems by implicitly considering the dependency of link travel times based on GPS trajectory data of vehicles. For example, Yang et al. (2018) used joint distributions to capture the travel time dependencies among candidate or partial paths by using sparse trajectory data. However, it is unknown if these methods can model effectively the dependency required for handling the investigated SSPs. To reflect the spatial and temporal correlations, the most general way to describe the link travel times is in the form of the joint probability distribution of all random travel time variables, which is generally represented by a set of stochastic scenarios (or support points) (Gao, 2005; Wang et al., 2020). A scenario represents one possible realization of travel speeds on all road links in all time periods. Previous SSP studies adopted sampling-based methods to handle the spatial and temporal correlations of speeds (or travel times). Zockaie et al. (2013) sampled 1,000 scenarios from a multivariate normal distribution using the Monte Carlo method. Yang and Zhou (2014) took 10 days of real link travel times from the freeways of San Diego as scenarios. Zockaie et al. (2016) generated 86 scenarios using the traffic simulator, DYNASMART-P (Mahmassani and Sbayti, 2009), based on 86 days of historical data on network-wide demand levels, weather conditions, incidents, and routing strategies in downtown Chicago. Huang and Gao (2012) sampled 50 scenarios (or support points) for link travel times from an assumed truncated multivariate normal distribution.

These previous studies simply pick an arbitrary number of scenarios and do not evaluate the effectiveness of the sampled scenarios. On one hand, it is well-known that sampling-based methods usually need a large number of samples to reflect the distribution of the random variables well, which leads to a long computation time. In some real-world applications such as path selection and routing in emergency rescue as well as on-demand and autonomous mobility environments, it is critical to handle SSP problems with a high computational efficiency. On the other hand, given historical data of the random variables, it is still not clear how to generate appropriate scenarios needed for SSP problems with spatially and temporally correlated speeds, except for using random sampling. It is also not clear how to evaluate the quality of the generated scenarios for different SSP problems.

Given the historical data of random variables, it is thus critical to investigate how many scenarios are needed to establish stable, trustworthy results based on sampling, and then propose a much more efficient method (i.e., one needing much fewer scenarios for the same quality of the results) based on explicit scenario generation for these SSP problems in real road networks.

The idea of the scenario generation method is to generate particular scenarios to approximate the original distribution, rather than picking samples

randomly as in the sampling-based method used in the existing SSP literature. The existing scenario generation methods can mainly be classified into four types (Homem-de Mello and Bayraksan, 2014), including the Quasi-Monte Carlo method (Wang and Tan, 2013), the sparse grid-based method (Chen et al., 2015), the moment-matching method (Høyland et al., 2003), and the probability metric-based method (Pflug, 2001).

However, we are going to handle a very high-dimensional distribution. The number of random variables in our paper is up to 37,500 (1250 links $\times$ 30 periods), which leads to a 37500×37500 correlation matrix. Due to huge memory requirements and unaffordable computation times, all these methods fail to generate reliable scenarios for such a high-dimensional problem within reasonable time. In particular, the first three scenario generation methods need to directly perform factorization operations of a huge correlation matrix when the quasi-Monte Carlo and sparse grid-based methods transform the original distribution to a distribution on the unit cube $[0, 1]^d$ and the moment-matching method corrects correlations. The probability metric-based method solves an optimization problem to minimize the distance metric between the scenarios and the original distribution. The four methods are all computing intensive, because the high-dimensional matrix operations in the first three methods are very costly in time and space and the optimization problem addressed in the fourth method is typically non-convex and NP-hard (Löhndorf, 2016). Moreover, the error bounds for the quasi-Monte Carlo and sparse grid-based methods increase with the dimensionality (Holtz, 2010), and the variance of the scenarios generated by the probability metric-based method deviates more and more from the variance of the original distribution as the dimensionality increases (Löhndorf, 2016). That is, in handling such high-dimensional distributions in SSPs, the scenarios generated by these methods inevitably lead to large errors and cannot represent the original distribution well.

Different from the above methods, Kaut (2014) proposed a copula-based scenario generation method by modelling the marginals and the copula separately. This is a promising method to handle our high-dimensional distributions because it avoids directly operating the huge correlation matrix and solving complex optimization problems. In a recent work by Guo et al. (2019b), this scenario generation method has been used successfully to handle spatially and temporally correlated stochastic speeds in vehicle routing problems on a simplified map of Beijing. For the investigated vehicle routing problem with the expected overtime minimization objective, only 15 scenarios (much less than the number required by random sampling) are needed to achieve an objective-function evaluation stability of 1% for a case with 142 nodes, 418 road links and 60 time periods, leading to over 25,000 correlated random speeds. It is still open if this method works for the realistic stochasticity of travel speeds in real road networks because their study assumed simplified distributions and correlations of travel speeds.

Following Guo et al. (2019b), this paper investigates various SSP problems with spatially and temporally correlated speeds based on real travel speed data from a freeway network and an urban road network (Guo et al., 2020). We

propose an effective method to generate scenarios for investigated SSP problems by integrating the copula-based scenario generation method with a stability test method. We find that whatever the correlation structure, there is a much better way to find scenarios than by using random sampling. We demonstrate that whether the goal is to obtain maximal quality for a given number of scenarios (because there is a limited execution time available), or a certain quality for a minimal number of scenarios (because accuracy is important), the copula-based scenario generation method is substantially better.

This paper contributes to the SSP literature from both technical and managerial perspectives. The technical contributions include (1) developing an effective and efficient methodology to construct reliable scenarios for handling SSPs with spatially and temporally correlated travel speeds, and (2) integrating the copula-based scenario generation method (Kaut, 2014) with a test for stability and introducing them to the SSP area for the first time. The managerial contribution is twofold. First, we found that different characteristics of SSPs (different O-D pairs, objectives, and road networks) affect the required number of scenarios to achieve a certain accuracy. Second, we found that the number of scenarios needed in an urban road network generally is larger than that in a freeway network.

This paper is organized as follows. In Section 2, the realistic stochasticity of spatially and temporally correlated travel speeds is introduced. Scenario generation and solution evaluations are discussed in Section 3. Then, Section 4 shows the experimental results and analyses with different O-D pairs and different objective functions in a freeway network. Section 5 describes the results of similar experiments conducted in an urban road network and summarizes the results from both road networks. In Section 6, conclusions are made and future research directions are discussed.

2. Data-driven stochasticity of spatially and temporally correlated travel speeds

To understand how travel speeds vary over time and space in real road networks, Guo et al. (2020) have investigated their marginal distributions and correlations, based on two travel speed datasets. The first dataset was a 110-day dataset collected from the road network of Chengdu city with 1,902 nodes and 5,943 directed links, which contains a total of 196,119,000 travel speed records from 300 2-min time periods per day. The second dataset was a 102-day dataset collected from the California freeway network (as shown in Fig. 1) with 168 nodes and 438 directed links, which consists of a total of 3,216,672 travel speed records from 72 5-min time periods per day.

Guo et al. (2020) found that about 94% of random travel speeds obeyed the normal distribution in the urban road network, while more than 93% of random travel speeds obeyed four different distributions in the freeway network, including normal (58%), Gumbel (24%), lognormal (6%), and beta (6%). These distributions were fitted based on the travel speed data after outliers of travel speeds were removed. However, some outliers were speeds close to zero on roads

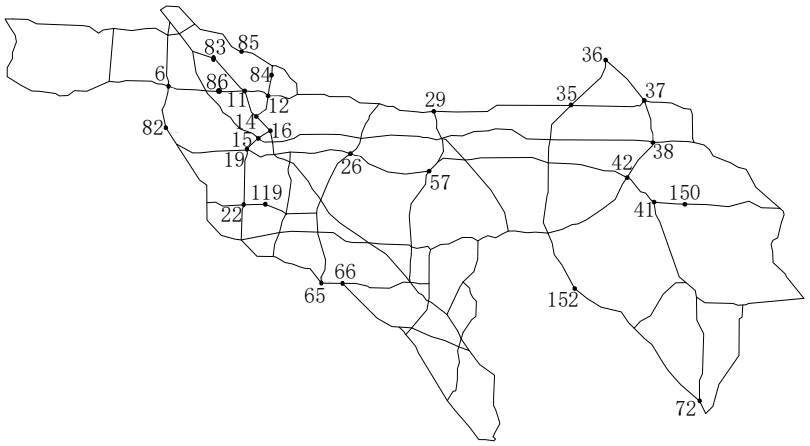

Fig. 1. Freeway network around Los Angeles. The numbers refer to nodes that we use in the main text.

that normally had more or less free float, which are usually not errors since they do represent real travel speeds. If the outliers were not removed, some random speed variables, about 1% in the urban road network and about 7% in the freeway network, could not be fitted well with these parametric distributions. Moreover, even if each speed variable can be fitted with a parametric distribution, it does not mean that the fitted distribution is the right one for the variable unless it is known what distribution family the speed data comes from. Therefore, when we later in this paper need marginal distributions, we use the empirical marginal distributions directly without trying to fit parametric distributions to the data, as our methodology allows the direct use of empirical distributions.

Guo et al. (2020) also found that correlations of travel speeds generally decreased with an increased distance in time and space, and about 27-42% (53-57%) of spatial-temporal correlations were significantly positive in the urban road (freeway) network. These results are just statistical results. They have not reported the correlation results of separate links and the corresponding reasons. Next, we take a link (14, 11) from the same freeway network as an example to present how the correlations of a single link vary over time and space using the same freeway speed dataset. Except for the three 2-hour time ranges (i.e., 8:00-10:00, 12:00-14:00 and 17:00-19:00) considered in Guo et al.'s work (2020), we further consider three more time ranges, including 10:00-12:00, 14:00-16:00, and 16:00-18:00.

Fig. 2 presents the spatial correlations between link (14, 11) and all other links in the network shown in Fig. 1 in six different time periods. In this figure, the correlations between the two horizontal lines that are parallel with the x-axis are statistically insignificant with a significance level of 0.05, and the red crosses represent the correlations between link (14, 11) and its 11 neighbouring

links (links sharing node 14 or 11). We see that, in a given time period, the travel speeds on link (14, 11) could be either significantly or insignificantly correlated with those on its neighbouring links. This finding holds true on all 30 randomly chosen links we observed. Also, the travel speeds on two neighbouring links could have significantly positive or negative correlations. For example, the speeds on link (14, 11) are significantly positively correlated with the speeds on link (16, 14) in four time periods 10:00-10:05 (0.37), 12:00-12:05 (0.47), 14:00-14:05 (0.43), and 17:00-17:05 (0.43). In addition, the speeds on link (14, 11) and its neighbour (12, 14) are negatively correlated (-0.22) in time period 8:00-8:05. The reason is simple. The two links and link (12, 11) form a triangle. A fair number of vehicles that head from node 12 to node 11, tend to choose the detour via node 14 when link (12, 11) is congested and link (12, 14) looks faster. However, these vehicles could slow down link (14, 11) since many vehicles are travelling on this link. Contrariwise, rather few vehicles going from node 12 to node 11 choose the detour via node 14 if link (12, 14) gets slower, resulting in fewer vehicles and thus higher speeds on link (14, 11). Both cases lead to a negative correlation between (12, 14) and (14, 11). Moreover, when the traffic on two neighbouring links is in opposite directions, the link travel speeds could be significantly negatively correlated as well. An example is given by the correlation (-0.37) of travel speeds on link (14, 11) and link (11, 14) in time period 16:00-16:05. Similar correlation findings have also been reported in the literature (Rachtan et al., 2013; Guo et al., 2019a).

Fig. 3 exhibits the temporal correlations of link (14, 11) between the first time period and all following time periods in six different 2-hour time ranges, where the stars in dashed lines represent statistically insignificant correlations with a significance level of 0.05. It is clear that, with the increase of time distance between two time periods, the temporal correlation on one link between the two time periods decreases on the whole. And the travel speeds on link (14, 11) in two immediately neighboring time periods could have strong positive correlations. We also calculate the temporal correlations on other 30 randomly chosen links in the same six 2-hour time ranges. We find only one single (insignificant) negative temporal correlation. These results are in line with the findings of Cheng et al. (2012) and Rachtan et al. (2013).

Fig. 4 exhibits the correlations between travel speeds on link (14, 11) in the time period 14:00-14:05 and speeds on its 11 neighbouring links in the 12 time periods within the time range of 14:00-15:00. We see that the correlation between link (14, 11) and each neighbouring link gradually changes over the time lag between the two time periods. For example, its correlation with link (14, 12) first increases gradually to a large value (0.42) in the period 14:15-14:20 and then decreases gradually to a small value (0.14) in the last period 14:55-15:00. The reason for this gradual change is that, as observed above, there exists a strong positive correlation between two travel speeds on a given link in some immediately neighboring time periods. As a result, the correlations between both of the two speeds and the travel speed on link (14, 11) in the period of 14:00-14:05 are close. It leads to a small change of correlations between two close-by periods for link (14, 12) in Fig. 4.

On the other hand, there may be a large positive correlation between the travel speeds on two neighbouring links separated by several time periods, such as the correlation 0.42 corresponding to link (14, 12) in period 14:15-14:20 in this figure. This is because the vehicles that head from node 14 to node 11, tend to choose the detour via node 12 when they observe that link (14, 11) is congested and link (14, 12) looks faster. But, there may be a time lag between the beginning of congestion (or no congestion) on link (14, 11) and the time when the vehicles observe the congestion (or no congestion) and choose (or not) to detour through link (14, 12). That is, although the travel speeds on link (14, 11) become high (or low) in period 14:00-14:05, it takes two 5-minute periods to significantly affect the speeds on link (14, 12).

In summary, there are large and statistically significant correlations among the link speeds in the road networks, thereby confirming that handling correlations in SSP calculations is meaningful and potentially important.

3. Scenarios generation and solution evaluation

3.1. Scenarios generation

Having the speed data, we need to generate appropriate scenarios for our calculations. We have chosen to approach the problem as follows. We take our speed dataset – see Section 4.1 for details – and view its empirical distribution as the true distribution of speeds. Obviously, the set is actually a sample from an underlying unknown distribution (or process), but it is beyond the goals of this paper to discuss the relationship between this empirical distribution and the true one. In this way we are in line with the literature (Yang and Zhou, 2014; Zockaie et al., 2016; Gu et al., 2019).

The base case will be sampling from the empirical distribution of random travel speeds. So whatever number of scenarios we need, we shall randomly pick that number of scenarios from the empirical distribution. We shall refer to this as RS (random sampling). Our base case does not take the sampling from estimated parametric distributions and the reasons are as follows. Going via estimated distributions may appear to provide more stable results, but that is only the case relative to the estimated distribution. Unless it is known what distribution family the speed data comes from, estimating a parametric distribution based on the speed data before sampling amounts to adding noise to the process. In our speed datasets, we do not know the distribution family (we do not even know if the data comes from a stable distribution). Even if we knew the distribution family, it would be very difficult (close to impossible) to estimate a reliable joint distribution for such a high-dimensional distribution (our biggest case has 37,500 dependent random speed variables). Moreover, if it was to be done, the number of speed data points would need to be enormous. Otherwise, the result would just be noise.

The alternative, which will turn out to be much better, will be based on explicit scenario generation. We shall denote this SG (scenario generation). We use the method in Kaut (2014) to generate scenarios of travel speeds. This

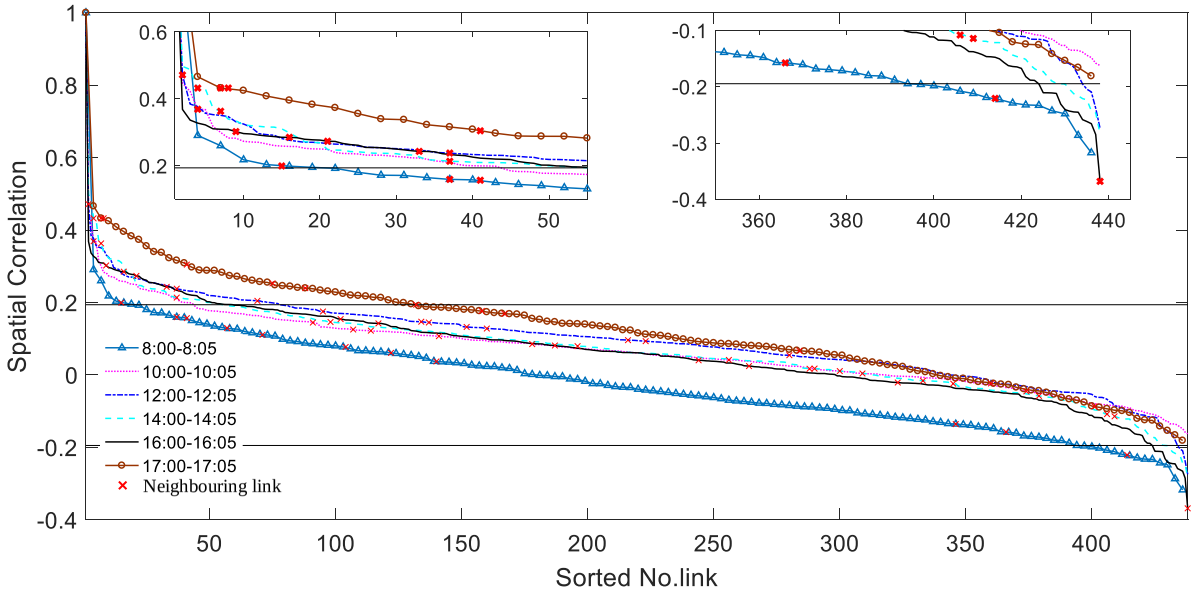

Fig. 2. The spatial correlations of link (14, 11) with other links in the road network in six time periods. For the curve of each time period, the link numbers are sorted in the decreasing order of spatial correlations. The red crosses represent the correlations between link (14, 11) and its 11 neighbouring links (links sharing node 14 or 11). The correlations between the two horizontal lines that are parallel with the x-axis are statistically insignificant with a significance level of 5%, the rest are significant.

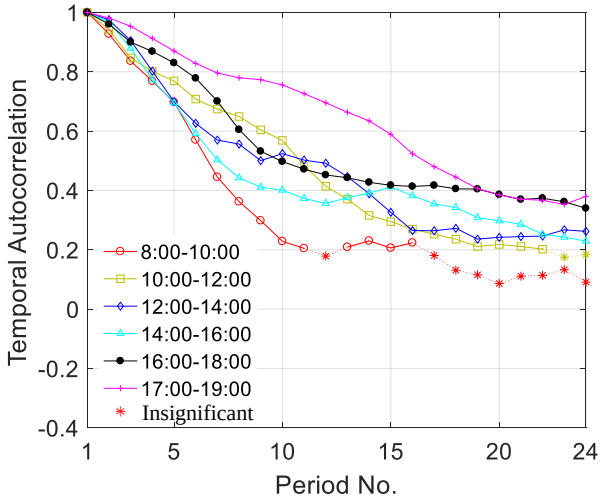

Fig. 3. The temporal correlations of link (14, 11) in six time ranges. The stars in dashed lines are not significant at the 5% level, the rest are.

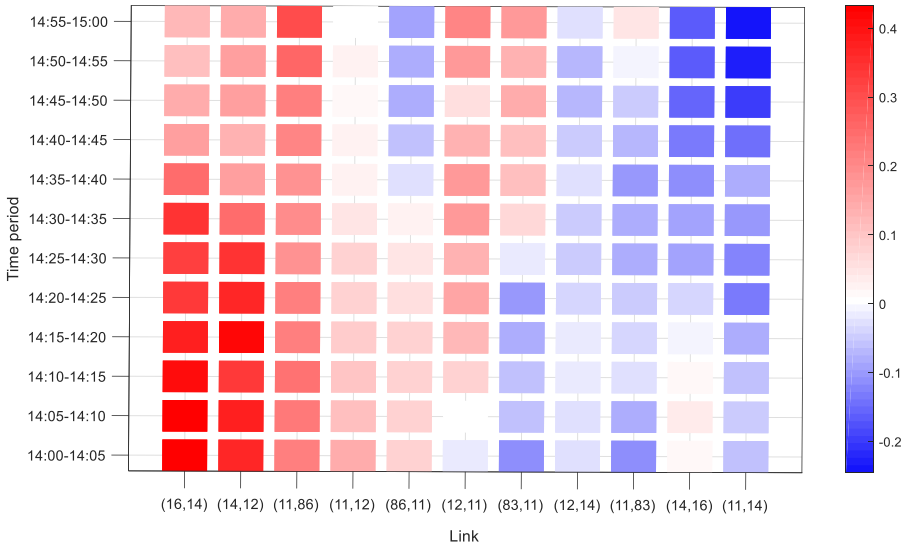

Fig. 4. The correlations between travel speeds on link (14, 11) in the first time period (14:00-14:05) and speeds on its 11 neighbouring links in the 12 time periods between 14:00-15:00.

method is based on Sklar's theorem (Sklar, 1973), showing that every multivariate distribution function is fully specified by its marginal distributions and its copula. A copula is a multivariate cumulative distribution function on the unit cube $[0,1]^d$ with uniform marginals, which describes the dependence between the random speed variables. In other words, modelling the dependencies of travel speeds can be fully decoupled from modelling the marginal distributions. However, since multivariate copulas are difficult to work with, the method approximates the multivariate copula by a set of bivariate copulas. By doing so, we move from one correlation per pair of random variables of travel speeds, which is what we mostly find in the literature, to one cumulative distribution function per pair. Clearly, using bivariate copulas is more powerful than using just correlations, although it cannot model higher-order dependencies and, hence, the complete dependency. However, this will decrease the numerical complexity from $O(S^n)$ to $O(n^2S^2)$ (Kaut, 2014). Correlations and bivariate copulas are closely related since the only parameters needed for normal copulas are the correlations. However, we are not estimating correlations directly, we are using the empirical copula as a starting point. We outline the basics of this approach in Appendix A.

The scenarios for random speed variables in the road network are generated in two steps: first, the method constructs a "scenario copula" as close to the empirical speed copula as possible, then the scenarios are transformed to the target marginal distributions for all random speed variables. Both the copula and marginal distributions can be specified using parametric families, or taken directly from provided speed data. In our case, the bi-variate copulas and marginal distributions are taken directly from the empirical speed distribution. The method uses randomness as a tie-breaker if a tie appears in an assignment in the method. The method thus generates the same or very similar scenarios in two different runs with the same input. This contrasts it with sampling where this is not the case.

A scenario set is always an approximation of travel speeds in the road network; that is in fact the whole point. Although sampling has very nice limit properties, the quality of a sampled set of scenarios can be rather bad, even the scenario means will be off. The scenario sets generated by the method we use always have means equal to the means of the given distribution, since we have full control of the discretization of the marginals. As a result, the mean of travel times on each link and each path are correct in these scenarios. For all other distributional properties, both RS and SG offer approximations. The feasibility and effectiveness of using bivariate copulas will be validated by extensive numerical experiments presented in Sections 4–5. We shall see that SG outperforms RS by a large margin.

3.2. Evaluation measures and stability

The chosen scenarios can have great impacts on the best solution to routing problems with spatially and temporally correlated stochastic travel times (Huang and Gao, 2018). It is thus critical to assess the quality of a set of sce-

narios. We shall test the qualities when scenarios of travel speeds come from both RS and SG.

We use two related measures, including relative difference RD and variance VAR, to assess the stability / quality of the set of scenarios. These two measures come from the in- and out-of-sample stability tests of Kaut and Wallace (2007) and work by generating and comparing multiple scenario sets. However, since the copula-based scenario generation method generates the same or similar scenario sets with the same inputs in different runs, the common in-sample stability test is not applicable here. Thus, we use a variant of the standard approach; to represent the case with S scenarios of travel speeds, we generate $2m+1$ scenario sets with size $S-m, S-m+1, \ldots, S, \ldots, S+m-1, S+m$, where m is an integer and set as 4 in our paper, based on tests in Guo et al. (2019b). For each scenario set of travel speeds, we take the problem at hand (in our case the SSP problem) and use a solution method from the literature to find an optimal (or near-optimal) solution. Then, there are $2m+1$ best solutions X_{S+i} for $i \in [-m, m]$. Calculate the objective value corresponding to each solution X_{S+i} based on each of these $2m+1$ scenario sets.

Let $F^+(X_{S+i})$, $F^-(X_{S+i})$ and σ_{S+i} be the maximum, the minimum and the variance of the $2m+1$ objective values corresponding to X_{S+i}. Then we calculate RD and VAR of the scenario set of travel speeds as follows:

$$RD = \max_{i \in [-m,m]} \left(\frac{F^+(X_{S+i}) - F^-(X_{S+i})}{F^+(X_{S+i})} \times 100\% \right) \tag{1}$$

$$VAR = \max_{i \in [-m,m]} (\sigma_{S+i}) \tag{2}$$

For a given stability requirement, e.g., $RD \leq 1\%$ or $RD \leq 2\%$, the minimal S satisfying the requirement is set as the number of scenarios necessary to achieve the corresponding objective function stability for the investigated problem.

It is important to understand that by seeing the empirical distribution as the true distribution, we are favouring RS. With a reasonably large number of scenarios, relative to the number of outcomes in the empirical distribution, sampling scenarios from the empirical distribution, without replacement, would look much better than had we sampled from the underlying distribution (or alternatively from the empirical distribution with replacement). The scenario set from sampling without replacement would be "perfect" much faster than it would had we sampled from the underlying distribution (or sampled with replacement), while SG would not principally change. We shall see in Sections 4–5, that even so, SG is much stronger than RS.

Let X_{all} be the optimal solution to the investigated SSP problem using all scenarios (i.e., all real speed data). We finally use a measure, ORD, to check for the performance difference between the optimal solution based on scenarios generated by SG or RS and the optimal solution X_{all} based on all available scenarios. This measure makes sense in our case since we are able to optimally solve our problem with the full empirical distribution, though at considerable computational costs. So even though this test cannot be performed generally,

we use it here since it helps us understand what is going on. We might have that, for example, RD and VAR both behave well, but the objective function value converges to the wrong value. Let $F^{all}(X_{all})$ be the optimal objective value when all scenarios are used, and $F^{all}(X_{S+i})$ be the objective value of solution X_{S+i} evaluated with all scenarios (that is, the true value). ORD is calculated by using Eq. (3).

$$ORD = \frac{1}{2m+1} \sum_{i=-m}^{m} \frac{(F^{all}(X_{S+i}) - F^{all}(X_{all}))}{F^{all}(X_{all})} \times 100\% \geq 0 \tag{3}$$

For SG, this is a genuine issue because the method is not guaranteed to be unbiased. We shall see, though, that it behaves very well. The lower ORD is, the less S scenarios produce biased results, provided stability is established. For RS, the performance difference between $F^{all}(X_{S+i})$ and $F^{all}(X_{all})$ is only caused by sampling errors since random sampling is unbiased. To reduce the impacts of uncertainty coming from RS itself, we report the minimum, average and maximal values of RD and VAR in ten runs, each using $2m+1$ scenario sets (the same number as for SG), as the results for RS in Sections 4–5.

4. Test case and results in a freeway network

4.1. Case setting

Extensive experiments are conducted to investigate the stability of objective function evaluations using RS and SG and compare the performances of the two methods for investigated SSP problems. In these experiments, the SSP problem instances are defined on the freeway network around Los Angeles as shown in Fig. 1, and on the 102-day real travel speed data described in Guo et al. (2020). In the first dataset, the link travel speeds are obtained by processing speed readings of 3,417 detection stations over 102 days, from May 1 to September 22 in 2017 excluding weekends and holidays. There are 10,512 (438 links $\times$24 periods) random speed variables and 55,245,816 ($10,512 \times 10,511 \div 2$) distinct correlations in each 2-hour time range (i.e., 24 5-minute time periods). When using the copula-based scenario generation method, we obtain the marginal distribution of each random speed variable and the 55,245,816 distinct bivariate copulas of all random variables based on the 102-day speed data.

We use the method proposed by Hall (1986) to calculate the shortest paths in stochastic spatially and temporally correlated networks. This method is originally proposed to find the minimum expected travel time path in a stochastic time-dependent network, and we modify it to find the optimal paths for SSP problems with different objective functions. Specifically, this method is an improvement heuristic, which integrates the branch-and-bound method and the K-shortest path technique to iteratively look for feasible paths until the optimal path is obtained. At each iteration k, the method explores a new path P_k that has the k^{th} minimum possible travel time $g(P_k)$ using a K-shortest path method – Yen's method (Yen, 1971) in our paper, and then calculates the actual expected travel time $f(P_{k-1})$ of path P_{k-1}. $f(P_{k-1})$ is the expected value of P_{k-1}'s travel

Table 1. Details of the twelve chosen O-D pairs.

No.	O-D pair	Locations
1	(65, 35)	Heavy traffic area to light traffic area with long distance
2	(19, 150)	Heavy traffic area to light traffic area with long distance
3	(16, 29)	Heavy traffic area to light traffic area with short distance
4	(16, 26)	Heavy traffic area to light traffic area with shorter distance
5	(38, 15)	Light traffic area to heavy traffic area with long distance
6	(37, 66)	Light traffic area to heavy traffic area with long distance
7	(41, 82)	Light traffic area to light traffic area with long distance passing heavy traffic area
8	(152, 85)	Light traffic area to light traffic area with long distance not passing heavy traffic area
9	(22, 42)	Light traffic area to light traffic area with long distance not passing heavy traffic area
10	(57, 6)	Light traffic area to light traffic area with short distance passing heavy traffic area
11	(84, 119)	Light traffic area to light traffic area with short distance passing heavy traffic area
12	(36, 72)	Light traffic area to light traffic area with short distance not passing heavy traffic area

times in all S scenarios. Let τ denote the minimum expected travel time of all paths evaluated already. We have $\tau = \min\{f(P_1), \ldots, f(P_{k-1})\}$. Through exploring new paths iteratively, the optimal path with the minimum expected travel time can be found when meeting $\tau < g(P_k)$. The proof is straightforward. For $i \geq 1$, we have $g(P_k) \leq g(P_{k+i})$ and $g(P_i) \leq f(P_i)$ according to the K-shortest path method as well as the definitions of $g(P_i)$ and $f(P_i)$. If $\tau < g(P_k)$, τ is less than the minimum possible travel times $g(P_{k+i})$ of all paths not evaluated yet, which is thus less than the actual expected travel time of all these paths. Consequently, τ is the globally minimum expected travel time and its corresponding path is the optimal path. The method is a general framework to solve optimally the fast path problem with time-dependent stochastic travel times. This framework can be easily modified to solve SSP problems with other objectives by adapting the method of calculating $g(P_k)$ to different objective functions. Details of the original and modified methods can be found in Appendix B. Of course, other shortest path methods can also be used, a survey of which can be found in Gendreau et al. (2015). However, the shortest path method is not the focus of this paper.

Sections 4.2–4.4 will present the stability results for RS and SG from different perspectives, such as the effects of different O-D pairs and different objective functions, respectively, on the stability of function evaluations. The experiments are performed on a laptop with an Intel Core i7-8550U CPU @2.00GHz and 16 GB RAM.

4.2. Effects of different origin-destination pairs

We examine and compare the effects of different O-D pairs on the stability and performances of RS and SG first, based on 32 different O-D pairs. Here we only present the results of twelve representative O-D pairs on the basis of different O-D distances and whether the path passes heavy traffic areas. Details of the chosen O-D pairs are presented in Table 1. The other 20 O-D pairs lead to similar results, which can be found in the online supplementary documents.

In these experiments, the departure time is set to 8am during the morning rush hours. The objective function $F1$ is to minimize a linear combination

Table 2. $ORD(\%)$ values at different S generated by RS and SG for different O-D pairs.

No.	O-D pair	$S = 10$ RS/SG	$S = 15$ RS/SG	$S = 20$ RS/SG	$S = 25$ RS/SG
1	(65, 35)	0.86/0	0.29/0	0.31/0	0.18/0
2	(19, 150)	0.62/0.50	0.43/0.13	0.35/0	0.35/0
3	(16, 29)	0.23/0.26	0.08/0	0.10/0	0/0
4	(16, 26)	0.11/0	0/0	0/0	0/0
5	(38, 15)	0/0	0/0	0/0	0/0
6	(37, 66)	0.61/0	0.30/0	0.28/0	0.36/0
7	(41, 82)	0.38/0.08	0.22/0.07	0.20/0.09	0.16/0.12
8	(152, 85)	1.34/0	0.58/0	0.15/0	0.13/0
9	(22, 42)	0.07/0	0/0	0/0	0/0
10	(57, 6)	0.23/0	0.26/0	0/0	0/0
11	(84, 119)	0.56/0	0.36/0	0.38/0	0.33/0
12	(36, 72)	0.32/0	0.08/0	0/0	0/0

of mean (μ) and standard deviation (σ) of path travel times, and this problem is referred as the mean–standard deviation shortest path problem (Zhang et al., 2017). Let θ (generally larger than zero) denote a specified weight factor that represents the risk aversion to travel time variability, T^s the travel time (unit: second) of the travel path in the s^{th} scenario, and S the total number of scenarios. This objective (Objective Function 1) is formulated as follows.

$$F1 = \mu + \theta \cdot \sigma \tag{4}$$

with $\mu = \frac{\sum_{s=1}^{S} T^s}{S}$ and $\sigma = \sqrt{\frac{\sum_{s=1}^{S} (T^s - \mu)^2}{S}}$.

Fig. 5 compares RDs and $VARs$ for the twelve O-D pairs when θ is set to a typical value 1.27 (Noland et al., 1998). For each O-D pair, the four types of hollow (solid) markers represent the results of SG (RS) at four different values of S. Specifically, the three markers on each vertical line, from top to bottom, represent the maximum, the mean, and the minimum of RDs or VARs generated by RS in ten runs at a certain S. The numerical values of RDs and VARs in Fig. 5 are presented in Table C.1 of Appendix C. Table 2 presents the ORD results. Fig. 6 shows the number of scenarios required (S_{RD}) for different O-D pairs to achieve the specified RD goals for both methods. For RS, the number of scenarios needed is calculated based on the mean of RD values in ten runs (this also favours RS as compared to SG, since in a given setting one could end up with any of the ten cases without knowing the actual quality of the scenarios used). We let S start from 10 and increase in steps of 5.

It can be found from Figs. 5-6 and Table 2 that:

1. Whichever method is used, the RDs and $VARs$ reduce with the increase of S on the whole, although small fluctuations exist for some O-D pairs. These fluctuations are reasonable and acceptable, and are caused by the randomness or heuristic nature of RS and SG.

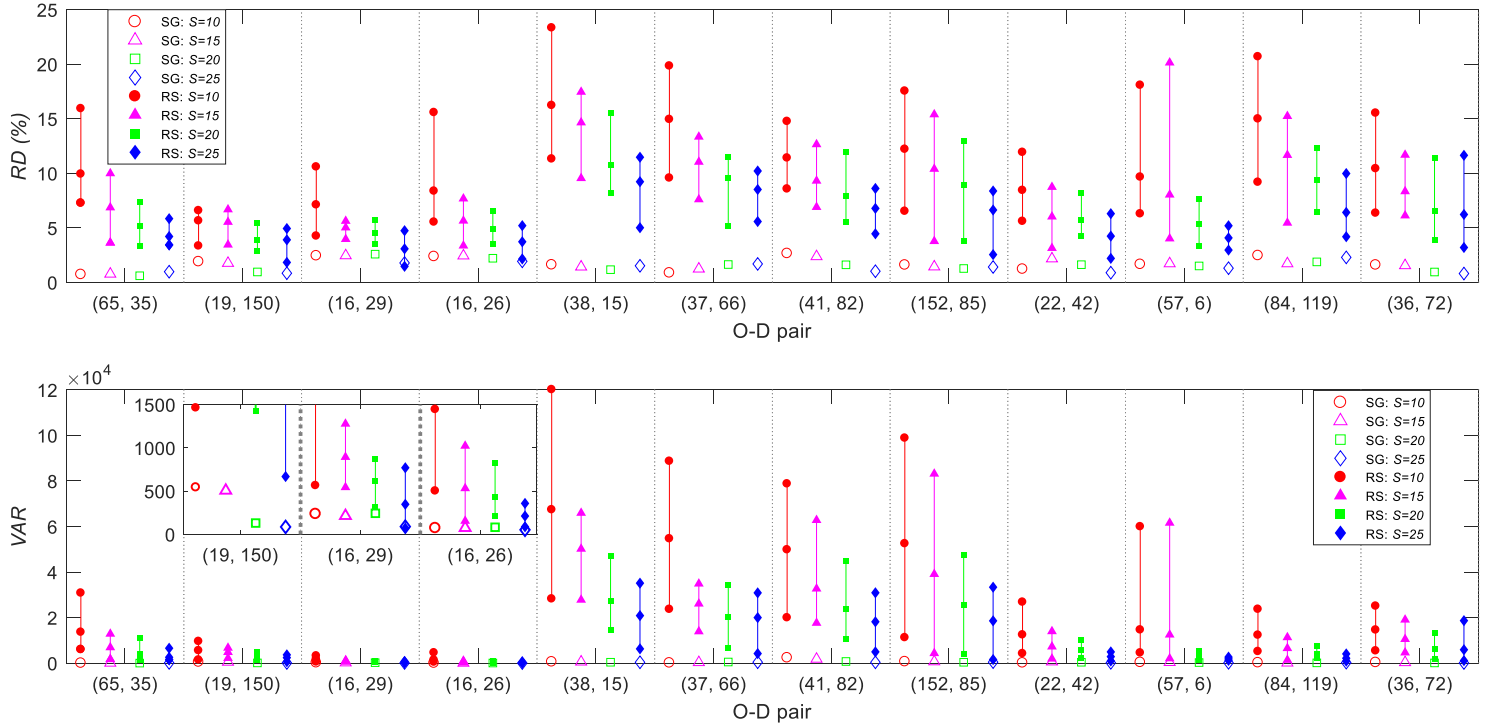

Fig. 5. Comparison of *RD* and *VAR* as generated by RS and SG for different O-D pairs. The three markers on each vertical line, from top to bottom, represent the maximum, the mean, and the minimum of *RD*s or *VAR*s generated by RS in ten runs at a certain S.

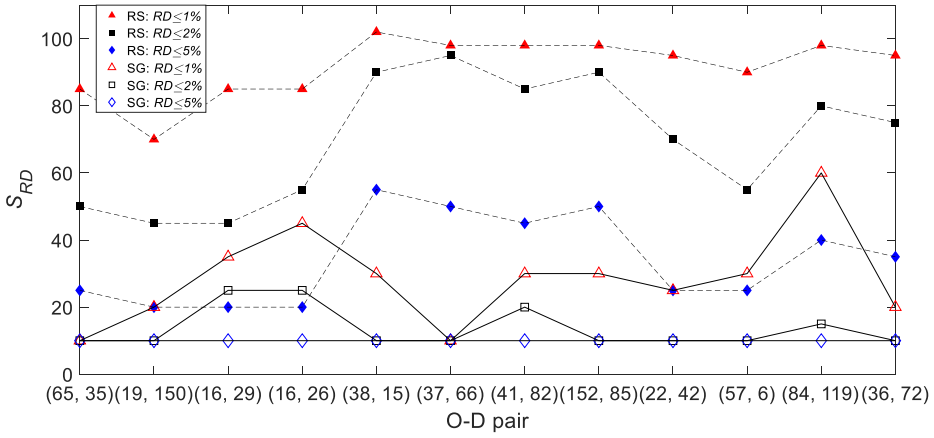

Fig. 6. Number of scenarios required by RS and SG for different O-D pairs and different stability levels.

2. For all O-D pairs, SG generates much smaller RDs and $VARs$ than RS, even for its minimal RDs and $VARs$. Taking O-D pair (37, 66) as an example, when S is equal to 10, the RD and VAR generated by SG are only about 9.23% and 0.72% of the minimal RD and VAR generated by RS. That is, with the same S (when it is not too large), the scenario set generated by SG leads to much more stable performance than RS for all investigated O-D pairs.
3. We see a few cases of ORD being positive for SG. However, except for (41, 82), it becomes zero as S increases within Table 2. For the O-D pair (41, 82), ORD goes to zero when S reaches 55 (not shown in the table). Hence, we see that SG does not produce biased results in our experiments, and the variation is caused by a not-yet-stable solution. We see throughout that ORD is much larger for RS than for SG.
4. As shown in Fig. 6, to achieve a stability level of 2% on objective $F1$, SG needs only 25 scenarios for all O-D pairs while the number of scenarios required by RS ranges from 45 to 95 (those are very large numbers as their maximum is 102).

4.3. Results of six objective functions

We further examine the effects of different objective functions on the performances of RS and SG by comparing these two methods based on six commonly used objective functions for all investigated O-D pairs. The departure time is set at 8am. The first objective is $F1$ formulated in Section 4.2 and the other five are described below. Objective functions $F1$ and $F6$ are travel time reliability criteria adopted in the literature.

Objective 2: Minimize the expected travel time $F2$.

$$F2 = \frac{\sum_{s=1}^{S} T^s}{S} \tag{5}$$

Objective 3: Minimize the expected carbon emission $F3$. Let e^s denote the carbon emission (unit: gram) of the travel path in the s^{th} scenario. The value e^s is calculated using the well-known MEET model (Hickman et al., 1999) with parameters for a gross vehicle weight of 3.5-7.5 tons, i.e., parameters K, a, b, c, d, e, and f are equal to 110, 0, 0, 0.000375, 8702, 0 and 0, respectively. N is the number of nodes in the network, and M is the number of time periods, with v_{ijt}^s representing the travel speed sample on link (i, j) in the t^{th} time period in the s^{th} scenario, and d_{ij} is the length of link (i, j). If the vehicle travels from node i to node j directly in time period t, x_{ijt} is equal to 1, otherwise it is 0.

$$F3 = \frac{\sum_{s=1}^{S} (e^s/1000)}{S} \tag{6}$$

with

$$e^s = \sum_{i=1}^{N}\sum_{j=1}^{N}\sum_{t=1}^{M}((K + a\cdot v_{ijt}^s + b\cdot {v_{ijt}^s}^2 + c\cdot {v_{ijt}^s}^3 + d/v_{ijt}^s + e/{v_{ijt}^s}^2 + f/{v_{ijt}^s}^3)\cdot x_{ijt})\cdot d_{ij} \tag{7}$$

Objective 4: Minimize the expected tardiness $F4$. Let L^s represent the tardiness in the s^{th} scenario, with D the given due time of arriving at the destination node and D_p the departure time from the origin node.

$$F4 = \frac{\sum_{s=1}^{S} L^s}{S} \tag{8}$$

with $L^s = \max(D_p + T^s - D, 0)$.

Objective 5: Minimize the expected sum of tardiness and earliness $F5$. Here W^s represents the earliness in the s^{th} scenario, while E is the given earliest time of arriving at the destination node.

$$F5 = \frac{\sum_{s=1}^{S} (L^s + W^s)}{S} \tag{9}$$

with $L^s = \max(D_p + T^s - D, 0)$, and $W^s = \max(E - T^s - D_p, 0)$.

Objective 6: Minimize the travel time budget $F6$ for a specified on-time arrival probability α, which is referred as the α-reliable path problem (Chen et al., 2018) or the minimal percentile travel time path problem (Yang and Zhou, 2017). A risk-averse decision-maker would prefer a larger α for a more reliable path.

$$F6 = \overline{T} \tag{10}$$

s.t.

$$Pr\{T^s \leq \overline{T}\} \geq \alpha \tag{11}$$

Specifically, based on discrete scenarios, the calculation of $F6$ for a path is conducted as follows. First, the travel time T^s in each scenario is calculated and ranked in an increasing sequence as $T^{s'_1} \leq T^{s'_2} \leq \ldots \leq T^{s'_S}$. Then, the value of $F6$ is equal to $T^{\overline{s'}}$, where $\overline{s'} = \min\{s' | \sum_{i=1}^{s'} p_i \geq \alpha\}$ and p_i is the possibility of i^{th} scenario. That is, the value of $F6$ is equal to the travel time in the $\overline{s'}^{th}$ scenario (Yang and Zhou, 2017).

To compare the results for different objective functions, we take O-D pair (65, 35) and departure time D_p at 8am as an example. Fig. 7 shows the ratios of RD and VAR generated by RS and SG for different S. The ratio of RD (VAR) is defined as the RDs (VARs) generated by RS divided by the corresponding RDs (VARs) generated by SG. The three markers on each vertical line, from top to bottom, represent the maximum, the mean, and the minimum of RD or VAR ratios in ten runs of RS at a certain S. The numerical values of RDs and VARs in Fig. 7 are presented in Table C.2 of Appendix C. Fig. 8 presents the number of scenarios required in each case. We set θ to 1 in $F1$, due time D to 8.88 (i.e., 8:52:48 in HH:MM:SS format) in $F4$, time window (E, D) to (8.78, 8.87) in $F5$, and on-time arrival probability α to 90% in $F6$. We set $\theta = 1$ in $F1$ so that the results of $F1$ here are consistent with the results of different θ shown in Table D.1, which corresponds to the experiments of studying the effects of different θ values in Section 4.4. Other O-D pairs produce similar results, which are detailed in the online supplementary documents.

It can be found from Figs. 7-8 that:

1. The objective function matters for the ratios for RD and VAR. We see that the ratios can be substantial for many objective functions, which indicates that SG produces much more stable results than RS. The observed values across different objective functions are not directly comparable, but still indicates well the dangers of using pure sampling.
2. To achieve specified RD goals, different objective functions require different numbers of scenarios. For objective functions $F2$ and $F3$ that calculate means, to achieve $RD \leq 1\%$, SG needs only 10 scenarios while RS requires more than or equal to 75 scenarios, and more similar results can be found in Appendix C. For the objective functions $F4$ and $F5$ that consider earliness and / or tardiness, both SG and RS need many scenarios, however, SG needs fewer scenarios to achieve $RD \leq 1\%$ than RS needs to achieves more loose $RD \leq 5\%$.

4.4. Effects of parameters in different objective functions

Since the objective functions $F1$, $F4$, $F5$ and $F6$ are directly affected by their parameter values, we now study the effects of these parameters on RD, VAR and ORD results. We conduct experiments for all O-D pairs. For each O-D pair, we customize the values of parameters to investigate as many settings as possible, and then obtain some general observations from the experimental results.

Take O-D pair (65, 35) as an example. The details of the experimental results are shown in Appendix D. We have the following observations:

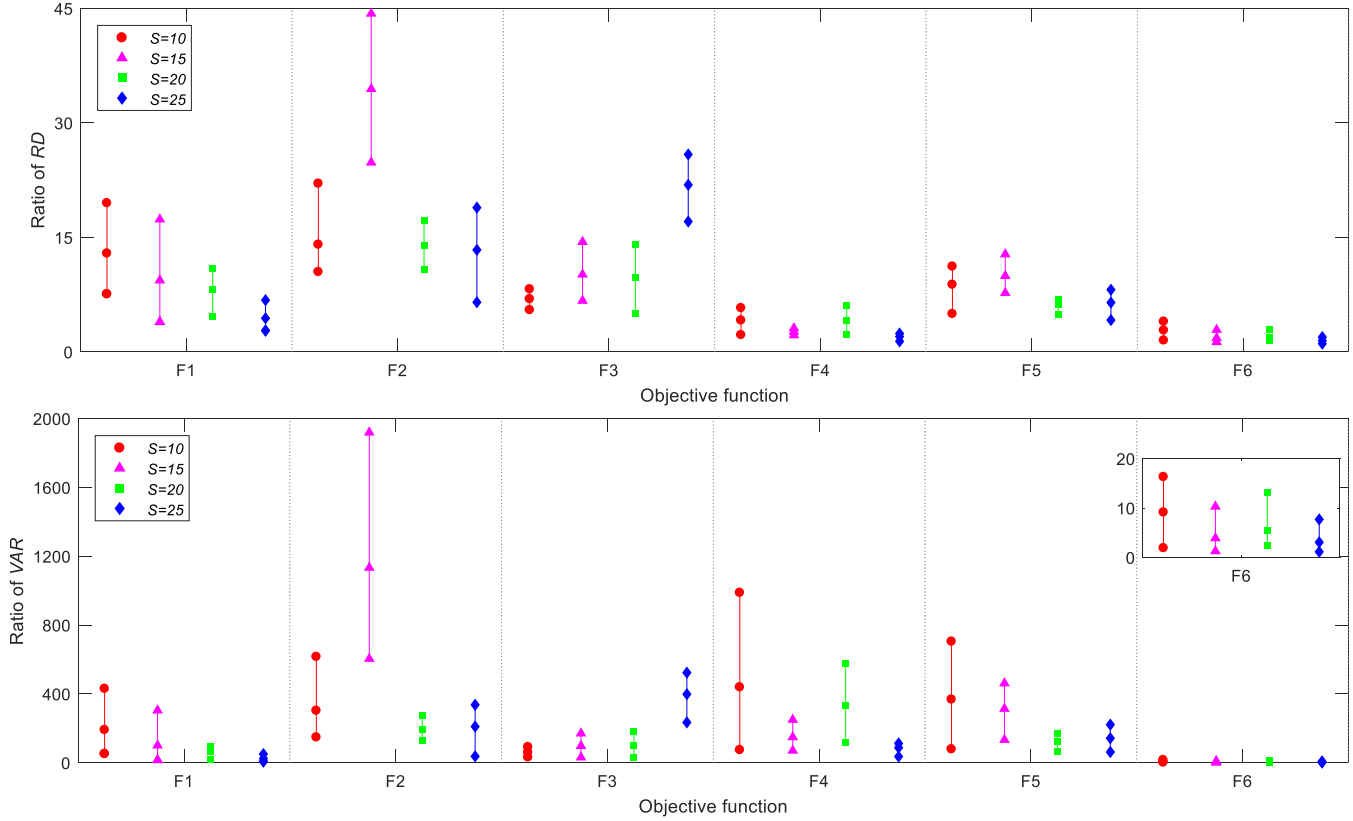

Fig. 7. Ratios of RD and VAR generated by RS and SG at different S for O-D pair (65, 35) and different objective functions. The three markers on each vertical line, from top to bottom, represent the maximum, the mean, and the minimum of RD or VAR ratios in ten runs at a certain S.

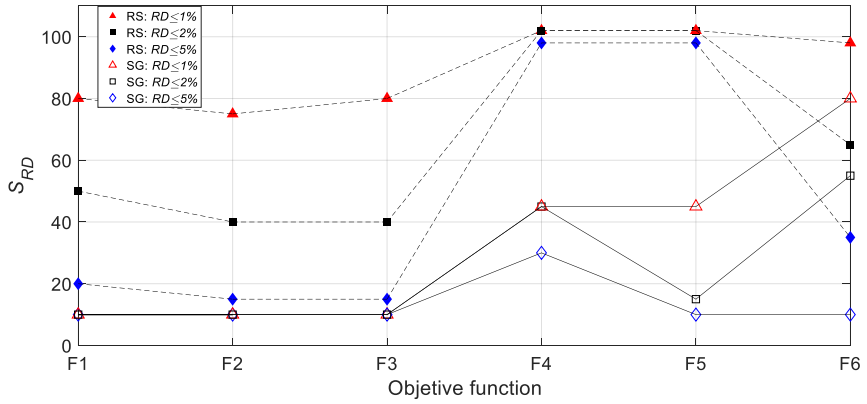

Fig. 8. Number of scenarios required by RS and SG for O-D pair (65, 35), when different objective functions and different stability levels are considered.

Table 3. Ranges of the ratio of RD and VAR generated by RS and SG with different parameters for O-D pair (65, 35) and $S = 10$.

	$F1$	$F4$	$F5$	$F6$
Ratio of RD	[8.70, 20.51]	[2.25, 11.93]	[1.44, 11.72]	[1.29, 4.64]
Ratio of VAR	[74.90, 393.06]	[105.82, 417.60]	[24.60, 444.80]	[1.36, 27.25]

1. RD and VAR generated by RS are much larger than those generated by SG throughout. This can be seen from Table 3, which presents the ranges of the ratio of RD and VAR under different parameters for O-D pair (65, 35) and $S = 10$. In the table, the minimal ratios of RD and VAR of all objective functions are larger than 1. This indicates that the scenarios generated by SG have more stable performance than those generated by RS for all these objective functions and parameters.
2. The values of RD and VAR can vary greatly in cases with different parameters. The results are not too surprising. When the objective is some kind of expectation, variation is much smaller than when the objective function depends on extreme values of the random variables. When extreme values are important, both methods, but particularly RS, will be very sensitive to what happens to be the extreme values in a scenario set. Detailed analyses can be found in Appendix D.
3. In most cases, we have $ORD = 0$. When it is not the case in the tables, the reason is that more scenarios are needed for stability. Eventually, all ORDs go to zero in our tests. In particular, that means that we never observe bias for SG — which generally is a possibility.

5. Test case from an urban road network and result summary

To examine the stability / quality of objective function evaluations of RS and SG and compare the performances of these two methods for the investigated SSP problems, Section 4 has presented extensive experimental and comparison results in terms of different O-D pairs and different objective functions. The findings aforementioned come from a freeway network. We further conduct similar experiments based on a link travel speed dataset from a larger urban road network (Guo et al., 2020). The number of random speed variables in the urban road network is 37,500 (1250 links $\times$30 periods), which is more than three times that in the freeway network used. The new experiments confirm that SG strongly outperforms RS in terms of stability for different O-D pairs and different objective functions. Details of experimental results from the urban network can be found in Appendix E.

Based on the results from the two road networks, we can draw the findings and have the managerial insights as follows.

1. SG strongly outperforms RS in terms of stability, i.e., in terms of RD and VAR. It is better to use the SG method to generate scenarios for the SSPs with spatially and temporally correlated travel times in real-world applications.
2. Different O-D pairs, as well as different objective functions and parameters could have large effects on the stability of objective function evaluations. This implies that a fixed number of scenarios for all cases, which is a common practice in the literature, would lead to unstable evaluations. Practitioners need to customize scenarios according to the characteristics of the SSPs.
3. For objective functions $F2$ and $F3$, SG needs only 10 scenarios for almost all cases to achieve an objective-function evaluation stability of 1% while RS usually needs much more in the freeway network. Therefore, when using SG, we can use the same number of scenarios (e.g., $S = 10$ in our cases) to handle the SSPs for all O-D pairs under $F2$ and $F3$ in this network. To determine the number of scenarios required, we could generally start with a small number (e.g., $S = 10$) of scenarios in the stability test and further increase it with a fixed step size (e.g., 5) to achieve a desired stability level.
4. For the other objective functions, sometimes much more scenarios are required to achieve a stability level of 1% because different parameter values could have a great impact on the RD results. However, SG always needs fewer scenarios than RS. In real-world applications, it is critical to generate scenarios separately for each case of the objective functions $F1$ and $F4-F6$, and we recommend starting with a large number of scenarios for these objective functions in the stability test.
5. The scenarios generated by SG are unbiased and the unbiased results ($ORD = 0$) can be achieved by a very small scenario size (e.g., S=10 for most cases) in the freeway network. This indicates that the feasibility and

effectiveness of using bivariate copulas to replace the multivariate copulas in scenario generation.

6. The urban road network leads to larger RD, VAR and ORD values than the freeway network does, which indicates that the number of scenarios required for the SSPs is larger in complicated urban road networks. The reason is simple. Compared with the freeway network, urban road networks have a more complicated network topology, shorter road links, and higher speed variance. They are thus characterized by higher correlations of travel speeds in both space and time. This could affect the number of scenarios required for the SSPs in urban road networks. But even so, SG always outperforms RS with a solid margin.

6. Conclusions

This paper addresses SSP problems with spatially and temporally correlated travel speeds based on real data from a freeway network and an urban road network. These problems involve correlated and very high-dimensional random speed variables.

We observe realistic stochasticity of travel speeds in a freeway network with 10,512 correlated random variables and 55,245,816 distinct correlations (or distinct bi-variate copulas). Taking a road link as an example, we investigate the spatial, temporal and spatio-temporal correlations of the travel speeds on separate links and analyse the corresponding reasons.

We then present two methods for generating scenarios for these high-dimensional SSP problems based on realistic stochasticity of travel speeds, one a copula-based scenario generation (SG) method and one a random sampling (RS) method. Extensive experiments are conducted to compare the performances of the two methods by examining the effects of different origin-destination pairs and different objective functions. In terms of two performance measures (RD and VAR), we show that SG needs much fewer scenarios than RS to achieve the same stability, typically about 6-10 times less for a stability level of 1% on objective function evaluations in the freeway network, despite the fact that we made several simplifying assumptions, all favoring RS. So, our main conclusion is that it is crucial how scenarios are generated, and in particular that random sampling is not a good idea unless the problem is small or execution time is of little importance. The suggested way of generating scenarios requires offline computations. We typically needed 28 minutes for 10 scenarios, up to 50 minutes for 25 scenarios when we had 10,512 random variables. The scenarios can then be reused as long as the map and the traffic intensity do not change. Our findings are helpful to handle effectively SSP problems with spatially and temporally correlated travel speeds in real-world applications where both computation efficiency and optimization performances are important. Typical application scenarios include path selection in emergency rescue as well as on-demand and autonomous mobility environment. Moreover, using our method, the existing SSP algorithms based on scenarios without consideration of correlations can be easily extended

to handle complex spatio-temporal correlations of link travel speeds in real road networks, which advances the SSP research.

This research is conducted in a freeway network and a small-scale urban road network. Our future research will improve the scenario generation method for applications in large urban street networks with higher speed variances and more path choices, and further consider partial correlations and partial autocorrelations. Another interesting direction is to investigate the effects of different correlations and / or complex multivariate copulas on the scenario performance and the solutions to SSP problems. Besides, it is also promising to use spatio-temporal graph neural networks to capture the spatial and temporal correlations of random speed variables, and develop effective methods to solve the SSP problems with spatially and temporally correlated travel speeds in the future.

Acknowledgements

Guo would like to thank the financial supports from the National Natural Science Foundation of China (Grant No. 71872118), the MOE (Ministry of Education in China) Project of Humanities and Social Sciences (Grant No. 18YJC630045) and Sichuan University (Grant No.s 2018hhs-37, SKSYL201819), Wallace thanks for the financial support from the Research Council of Norway (Grant No. 280536), and Zhang thanks for the financial support from the China Scholarship Council. Special thanks should also go to the Freeway Performance Measurement (PeMS) Project which provides the data in the empirical study.

Appendix A: Scenario generation method

This appendix outlines the major ideas behind the scenario generation method used in this paper. For more details, see Kaut (2014). The starting point is Sklar's theorem (Sklar, 1973), which shows that any distribution can be separated into marginal distributions and a copula, where the latter models how the random variables are connected, without a reference to the marginals. Hence, starting from an empirical distribution, we decide how many scenarios we want –S – and based on that create a discrete marginal distribution for each random variable involved, *with that number of outcomes*. Discretizing a one-dimensional distribution is straightforward, and we do not discuss that here. In particular, this allows us make sure that the expected value of each random variable is the same as in the empirical distribution.

If we have M sample points, we also have M different values in the marginal distribution for each of the N random variables. In the left part of Fig. A.1 we show an example of an empirical distribution with 100 points over approximately $[-2, 2] \times [-2, 2]$.

The next step is to remove the actual values for these points and only look at the ranks, i.e., each point is described by a pair (a, b) showing that a certain point contains the a'th lowest value of the first random variable and the b'th lowest of the other. So with 100 points, both a and b will take on all values from

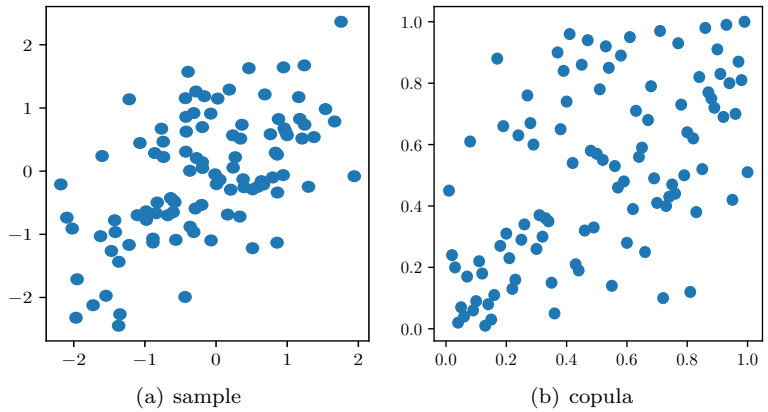

(a) sample (b) copula

Fig. A.1. Example empirical distribution and scaled ranks for 100 sample points.

1 to 100 exactly once. Since copulas are defined on $[0, 1]$ we scale the ranks just found on $[1, 100] \times [1, 100]$ down to $[0, 1] \times [0, 1]$. This gives us the right part of Fig. A.1. Notice that the right part is not a linear scaling of the left part, but rather of the ranks corresponding to the left part.

The point of the scenario generation procedure is now to find a copula for the scenarios, which is as close as possible to the the right part of Fig. A.1. We do that by minimizing a certain distance between the cumulative probability distribution function (cdf) for the copula in Fig. A.1 and the cdf for the copula of our scenarios. Assume we want five scenarios. We then take the $[0, 1] \times [0, 1]$ in the right part of Fig. A.1 and create a five by five grid instead also over $[0, 1] \times [0, 1]$. Then we find the proportion of points in each of the resulting 25 squares, forming a discrete bivariate distribution, see (a) and (b) in Fig. A.2. Part (a) corresponds to the right part of Fig. A.1, but with the 5×5 grid put on top. Part (b) then simply shows the result of this counting, given in proportions / probabilities. By accumulating the probabilities, we get the cdf of that distribution, shown in the last part of Fig. A.2, which serves as the target cdf for the scenario copula.

The copula we seek will then correspond to a rank over the 5×5 matrix (i.e., one dot in each row and one in each column) so that its cdf is as close as possible to the one given. For the distance, we use the sum of absolute values of the differences in each section of the grid, as shown in Fig. A.3. There, the distance is equal to the sum of grid values in the second part, i.e., 0.81.

In higher dimensions, we do not use the multi-variate copula, as its distance is difficult to compute. Instead, we use the heuristic from Kaut (2014), which works on bi-variate copulas. The heuristic adds one margin at a time and assigns the ranks consecutively to scenarios with the smallest distance in the copulas connected the new margin to the already assigned ones—see Fig. A.4 for a pseudo-code of this procedure (Kaut, 2014).

Calculation of the distance δ_{js}^k on line 5 of the algorithm is illustrated in

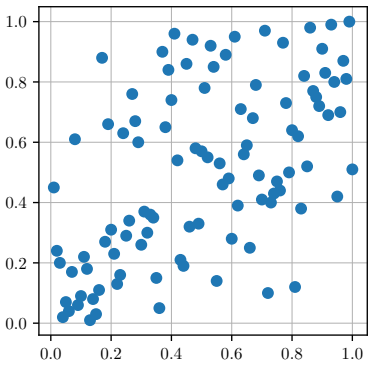

(a) Counting ranks

0.01	0.02	0.06	0.03	0.08
0.02	0.05	0.01	0.05	0.07
0.01	0.01	0.07	0.08	0.03
0.04	0.08	0.04	0.03	0.01
0.12	0.04	0.02	0.01	0.01

(b) Densities

0.2	0.4	0.6	0.8	1.0
0.19	0.38	0.55	0.68	0.8
0.18	0.34	0.43	0.51	0.6
0.16	0.28	0.3	0.37	0.4
0.12	0.16	0.17	0.19	0.2

(c) Accumulated probabilities

Fig. A.2. Target distribution for the scenario copula.

0.2	0.4	0.6	0.8	1.0
0.2	0.4	0.6	0.8	0.8
0.2	0.4	0.4	0.6	0.6
0.2	0.2	0.2	0.4	0.4
0.2	0.2	0.2	0.2	0.2

(a) Scenario cdf

0.0	0.0	0.0	0.0	0.0
0.01	0.02	0.05	0.12	0.0
0.02	0.06	0.03	0.09	0.0
0.04	0.08	0.1	0.03	0.0
0.08	0.04	0.03	0.01	0.0

(b) Absolute cdf differences

Fig. A.3. Scenario cdf and its distance from the target from Fig. A.2.

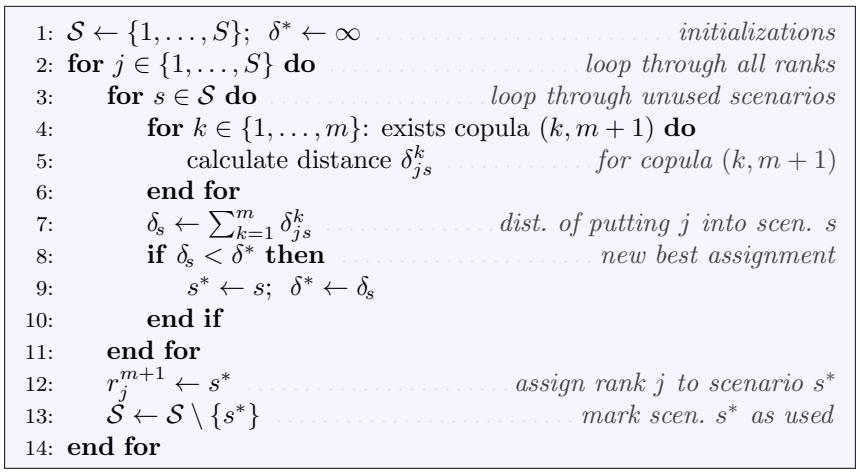

Fig. A.4. Step m of the multivariate heuristic: adding margin $m+1$ to the set of already generated margins $1, \ldots, m$. There, δ_{js}^k is the deviation in copula $(k, m+1)$, caused by assigning rank j (of margin $m+1$) to scenario s.

Fig. A.5, for copula used in the previous figures. Since this is a bi-variate copula, we have $m = 1$ (connecting second margin to the first one) and $k = 1$ is the only choice on line 4 of the algorithm. The figure shows assignment of the third rank ($j = 3$), with the first rank already assigned to scenario 1 and second rank to scenario 3—so $\mathcal{S} = \{2, 4, 5\}$; in particular, the figure shows the distance of assigning rank 3 into scenario 4, i.e., $\delta_{3,4}^1$.

Using only bi-variate copulas might seem limiting, but it is comparable to what is often done in the literature when looking at dependencies – looking at just correlations – and in fact is stronger than that as it picks up more information about the shape of the distribution than by using just correlations.

At this point, we have scenarios for the copula, instead of the target distribution. In particular, the margins consist of permutations of the set $\{1, \ldots, S\}$. To get the desired distribution, we need to scale the values into the $(0, 1)$ interval and then apply the inverse of the marginal cdf. For this, we divide $(0, 1)$ into S subintervals and apply the inverse cdf on their midpoints. Hence, the scenarios consists of conditional medians of the subintervals,

$$x_i^s = F_i^{-1}\Big(\frac{r_s^i - 0.5}{S}\Big),$$

where r_i^s is the rank of margin i in scenario s, and F_i is the margin's cdf. In case of a discrete cdf, such as the empirical cdf when using historical data, we follow Kaut (2014) and use cubic splines to smooth the cdf and make it invertible.

It may seem that this is just a complicated way to combine or accumulate outcomes in the empirical distribution. But it is not. By going from the left to the right part of Fig. A.1, and then using Sklar's theorem, we can use any available method to discretize the marginals, instead of letting them be a somewhat

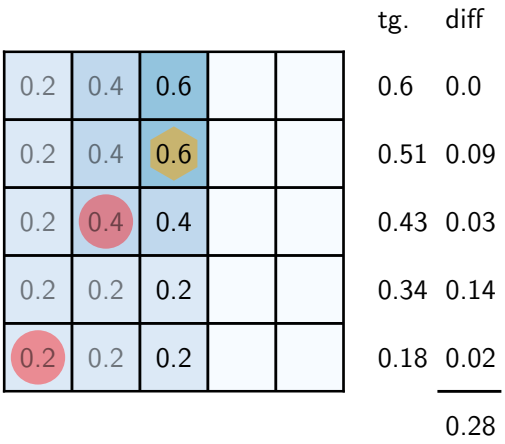

Fig. A.5. Calculation of distance δ_{js}^{k} from Fig. A.4, for the third margin from Fig. A.3. Note that the figure has ranks of margin 2 on x-axis and scenarios on y-axis, so its columns correspond to rows in the previous figures.

noisy result of the scenario generation procedure. In sampling, for example, a marginal distributions will amount to S sampled values, which for small S – which is what we need – can be rather noisy, even though, as the sample size increases the sampled distribution gets arbitrarily good. This is why this copula-based scenario generation is so much better than random sampling.

Table B.1. Framework of Hall's method (1986).

Step No.	DO
1	Set $k = 1$, $\tau = \infty$
	Find the shortest path P_1 with the minimum possible objective value $g(P_1)$
2	Set $k = k + 1$
	Calculate the actual objective value $f(P_{k-1})$ of P_{k-1}
3	Find the path P_k with the k^{th} minimum possible objective value $g(P_k)$
4	If $f(P_{k-1}) < \tau$
	$\tau = f(P_{k-1})$
	$P^* = P_{k-1}$
	If $\tau \geq g(P_k)$
	Return to Step 2
	If $\tau < g(P_k)$
	τ is the optimal objective value
	P^* is the optimal path
	Stop and return τ, P^*

Appendix B. Stochastic shortest path solving method

We use the method proposed by Hall (1986) to handle the SSP problems with different objective functions in stochastic spatially and temporally correlated networks. This method is originally proposed to find the minimal expected travel time path in a stochastic time-dependent network, and we modify it to find the optimal paths for our SSP problems with different objective functions.

Table B.1 shows the framework of Hall's method. At each iteration k, a new solution P_k (i.e., the path with the k^{th} smallest possible objective value) is found using a K-shortest path method – Yen's method (Yen, 1971) in our paper, and the actual objective value (τ) of the best possible path is updated. τ is the minimum of objective values of all $k-1$ paths evaluated already. That is, $\tau = \min\{f(P_1), \ldots, f(P_{k-1})\}$. Note that the method probably needs to explore and evaluate a large number of solutions to get the optimal one. However, the efficiency of this method is not the concern of this paper.

Next, we verify the optimality of the framework of Hall's method. As shown in Table B.1, $g(P_k)$ is the minimum possible objective value of path P_k, and $f(P_k)$ is the actual objective value of path P_k. We have $g(P_k) \leq f(P_k)$. When $\tau < g(P_m)$ at iteration m, we have $\tau < g(P_m) \leq f(P_m)$, that is, $\tau < f(P_m)$. Since $g(P_k) \leq g(P_{k+i})$ for all $i \geq 1$, we have $\tau < g(P_m) \leq g(P_{m+i}) \leq f(P_{m+i})$. That is, $\tau < f(P_{m+i})$ for all $i \geq 1$. Therefore, τ is not only the minimum objective value of all evaluated paths, but also less than the objective values of all unevaluated paths P_{m+i} ($i \geq 0$). τ is thus the global optimal objective value.

In summary, to get the optimal path in this framework, two conditions need to be satisfied: (1) $g(P_k) \leq g(P_{k+1})$ and (2) $g(P_k) \leq f(P_k)$. The first condition can be easily satisfied by using the Yen's method (Yen, 1971) to find the K-shortest paths optimally in a static and deterministic network. To meet the second condition, the key is to set the minimum possible objective value on

each road link, which has not been illustrated clearly in Hall's paper (1986). We set it for our SSP problems with different objective functions as follows. Since the method for $F2$ is the basis for other objective functions, we introduce it first.

$F2$: Minimize the expected travel time

We first find the maximum speed v_{ij}^{max} on each link (i, j) over all 24 time periods (2-hour time range) and all S scenarios, and then set the value of d_{ij}/v_{ij}^{max} as the minimum possible travel time on link (i, j).

Because v_{ij}^{max} is the highest possible speed on link (i, j), d_{ij}/v_{ij}^{max} must be less than or equal to the travel time on this link in any time periods and any scenarios. Therefore, the sum $g(P_k)$ of the minimum possible travel time on all links of path P_k must be less than or equal to the expected travel time $f(P_k)$ according to Eq. (5). This is, condition (2) holds.

$F1$: Minimize a linear combination of mean (μ) and standard deviation (σ) of path travel times

According to Eqs. (4)-(5), for path P_k, its objective value of $F1$ must be greater than or equal to the objective value of $F2$ since θ is generally equal to or bigger than 0. Therefore, we can directly use the minimum possible travel time for $F2$ as the minimum possible objective value for $F1$, which guarantees condition (2) holds.

$F3$: Minimize the expected carbon emission

The minimum carbon emission value e_{ij}^{min} over all time periods and all scenarios is set as the minimum possible carbon emission on the link. According to Eq. (6), the sum $g(P_k)$ of the values of e_{ij}^{min} on all links of path P_k must be less than or equal to the expected carbon emission $f(P_k)$ because e_{ij}^{min} is less than or equal to the carbon emission values on link (i, j) in any time periods and any scenarios. Condition (2) holds.

$F4$: Minimize the expected tardiness

To get the minimum possible tardiness for path P_k, the vehicle must travel each link at the maximum speed, which is consistent with objective function $F2$. Therefore, we use the same method for $F2$ to get the minimum possible travel time $T^{min}(P_k)$ of path P_k, and then the minimum possible tardiness $g(P_k)$ is set as $max(D_p + T^{min}(P_k) - D, 0)$.

According to Eq. (8), $g(P_k)$ must be less than or equal to the expected tardiness $f(P_k)$ because $T^{min}(P_k)$ is the minimum possible travel time of path P_k, as stated for $F2$. Condition (2) holds.

$F5$: Minimize the expected sum of tardiness and earliness

Here, we need to get the minimum possible tardiness and earliness respectively. The minimum possible tardiness $L^{min}(P_k)$ of path P_k is calculated using the same method for objective function $F4$. The minimum possible earliness $W^{min}(P_k)$ of path P_k can always be zero theoretically, as the vehicle could avoid earliness by lowering down the travel speed or temporary parking. Therefore, we set the $W^{min}(P_k)$ of path P_k as zero.

The sum $g(P_k)$ of $L^{min}(P_k)$ and $W^{min}(P_k)$ must be less than or equal to the expected tardiness and earliness $f(P_k)$ according to Eq. (9). Condition (2)

Table C.1. Numerical values of RD and VAR results shown in Fig. 5.

	No.	O-D pair	$S = 10$ RS/SG	$S = 15$ RS/SG	$S = 20$ RS/SG	$S = 25$ RS/SG
$RD(\%)$	1	(65, 35)	(7.28, 9.95, 15.94)/0.74	(3.64, 6.87, 10.00)/0.78	(3.33, 5.21, 7.42)/0.61	(3.44, 4.21, 5.85)/0.98
	2	(19, 150)	(3.35, 5.66, 6.59)/1.92	(3.45, 5.54, 6.69)/1.77	(2.84, 3.88, 5.48)/0.96	(1.84, 3.91, 4.94)/0.85
	3	(16, 29)	(4.26, 7.12, 10.60)/2.46	(3.97, 5.03, 5.63)/2.46	(3.50, 4.50, 5.71)/2.59	(1.48, 3.08, 4.74)/1.79
	4	(16, 26)	(5.54, 8.38, 15.58)/2.39	(3.37, 5.65, 7.68)/2.45	(3.49, 4.87, 6.54)/2.22	(2.15, 3.73, 5.21)/1.94
	5	(38, 15)	(11.33, 16.23, 23.35)/1.63	(9.55, 14.66, 17.46)/1.43	(8.18, 10.75, 15.55)/1.17	(5.02, 9.23, 11.48)/1.53
	6	(37, 66)	(9.58, 14.95, 19.85)/0.88	(7.61, 11.05, 13.35)/1.24	(5.21, 9.59, 11.5)/1.64	(5.58, 8.52, 10.22)/1.70
	7	(41, 82)	(8.58, 11.42, 14.77)/2.66	(6.91, 9.31, 12.65)/2.38	(5.53, 7.94, 11.99)/1.62	(4.46, 6.79, 8.62)/1.03
	8	(152, 85)	(6.54, 12.22, 17.55)/1.61	(3.78, 10.40, 15.40)/1.44	(3.84, 8.93, 12.98)/1.28	(2.55, 6.64, 8.38)/1.42
	9	(22, 42)	(5.61, 8.45, 11.94)/1.23	(3.15, 6.03, 8.74)/2.18	(4.22, 5.72, 8.20)/1.63	(2.21, 4.25, 6.30)/0.89
	10	(57, 6)	(6.30, 9.67, 18.09)/1.67	(4.02, 8.04, 20.14)/1.73	(3.37, 5.36, 7.64)/1.51	(2.97, 4.08, 5.20)/1.31
	11	(84, 119)	(9.20, 15.00, 20.70)/2.48	(5.46, 11.67, 15.24)/1.73	(6.43, 9.35, 12.30)/1.89	(4.19, 6.42, 9.98)/2.30
	12	(36, 72)	(6.36, 10.44, 15.53)/1.61	(6.13, 8.35, 11.69)/1.55	(3.86, 6.55, 11.45)/0.96	(3.20, 6.23, 11.65)/0.82
VAR	1	(65, 35)	(6047, 13658, 30847)/70	(1724, 6916, 12871)/91	(1319, 4156, 11125)/49	(1496, 2589, 6572)/122
	2	(19, 150)	(1464, 5565, 9605)/545	(2222, 4826, 6721)/507	(1426, 2684, 4998)/131	(669, 2425, 3672)/86
	3	(16, 29)	(566, 1791, 3259)/237	(544, 894, 1278)/214	(322, 612, 866)/244	(73, 348, 770)/90
	4	(16, 26)	(503, 1445, 4618)/74	(155, 532, 1023)/76	(215, 428, 820)/82	(88, 212, 358)/53
	5	(38, 15)	(28282, 67444, 120184)/638	(27798, 50188, 65956)/590	(14387, 27499, 47051)/418	(6297, 20887, 35141)/402
	6	(37, 66)	(23704, 54701, 88716)/170	(13921, 26106, 34894)/340	(6539, 20393, 34486)/524	(4230, 20013, 30885)/428
	7	(41, 82)	(20006, 49856, 78798)/2421	(17655, 32707, 62801)/1823	(10448, 23981, 44819)/752	(4974, 18188, 30921)/382
	8	(152, 85)	(11272, 52525, 98880)/717	(4353, 39106, 83156)/686	(4209, 25416, 47481)/404	(1597, 18596, 33372)/468
	9	(22, 42)	(4262, 12487, 26860)/187	(1933, 7259, 13977)/636	(2471, 5722, 10292)/415	(972, 2866, 4955)/154
	10	(57, 6)	(4570, 14668, 59985)/403	(2057, 12507, 61605)/373	(1193, 3377, 5210)/287	(1229, 1888, 2677)/174
	11	(84, 119)	(5180, 12358, 23734)/255	(1402, 6553, 11332)/144	(2195, 4051, 7619)/153	(903, 2184, 4074)/240
	12	(36, 72)	(5466, 14625, 25113)/357	(4642, 10547, 19070)/322	(1881, 6426, 13282)/123	(1123, 5918, 18681)/83

holds.

$F6$: Minimize the travel time budget for a specified on-time arrival probability α

As stated in Section 4.3, the objective value of $F6$ equals to the vehicle's travel time T_s in one of the S scenarios. Here, we use the minimum possible travel time generated for objective function $F2$ as the minimum possible objective value for $F6$ as well.

According to Eq. (10), the sum $g(P_k)$ of the minimum possible travel times on all links in path P_k must be less than or equal to the travel time in any scenarios $f(P_k)$ since the minimum possible travel time d_{ij}/v_{ij}^{max} on link (i, j) is less than or equal to the travel time on link (i, j) over all time periods and all S scenarios. Condition (2) holds.

Appendix C. Supplementary result

In this appendix, Tables C.1 and C.2 show the corresponding numerical values of RD and VAR results shown in Figs. 5 and 7, respectively. In these tables, the results generated by RS and SG for each S are separated by a slash. The three values for RS in each cell represent the minimum, the mean, and the maximum of RDs and VARs in ten runs at S. Given different O-D pairs, Tables C.3 and C.4 present the number of scenarios required to achieve the specified RD goals for both methods under objective functions $F2$ and $F3$, respectively.

Table C.2. Numerical values of RD and VAR results shown in Fig. 7.

	Objective function	$S = 10$ RS/SG	$S = 15$ RS/SG	$S = 20$ RS/SG	$S = 25$ RS/SG
$RD(\%)$	$F1$	(4.52, 7.7, 11.64)/0.60	(2.51, 6.00, 11.11)/0.64	(2.44, 4.30, 5.75)/0.52	(2.26, 3.56, 5.49)/0.81
	$F2$	(4.62, 6.20, 9.73)/0.44	(3.06, 4.25, 5.47)/0.12	(2.44, 3.14, 3.89)/0.23	(1.18, 2.42, 3.42)/0.18
	$F3$	(4.70, 5.93, 7.03)/0.85	(2.66, 4.02, 5.71)/0.40	(1.81, 3.51, 5.10)/0.36	(2.49, 3.19, 3.77)/0.15
	$F4$	(66.33, 82.42, 100)/4.96	(50.18, 68.31, 89.49)/1.40	(49.43, 61.14, 77.11)/2.52	(44.38, 54.41, 64.62)/2.03
	$F5$	(42.61, 53.2, 63.03)/4.45	(24.33, 44.11, 67.52)/1.25	(31.15, 38.53, 43.61)/2.26	(24.58, 29.63, 37.58)/1.82
	$F6$	(7.09, 13.25, 18.62)/4.67	(6.33, 8.88, 14.13)/4.88	(6.02, 7.31, 11.62)/3.87	(4.66, 6.35, 8.43)/4.33
VAR	$F1$	(2356, 8720, 19638)/46	(953, 6065, 18310)/60	(741, 2258, 3339)/35	(601, 1908, 4068)/81
	$F2$	(2365, 4831, 9820)/16	(1153, 2163, 3662)/2	(791, 1206, 1681)/6	(132, 751, 1204)/4
	$F3$	(0.39, 0.73, 1.11)/0.01	(0.12, 0.38, 0.67)/0	(0.07, 0.25, 0.45)/0	(0.13, 0.22, 0.28)/0
	$F4$	(784, 2252, 4859)/16	(316, 1263, 3017)/2	(282, 759, 1530)/6	(250, 475, 824)/4
	$F5$	(2678, 4448, 7732)/16	(590, 1806, 3897)/2	(703, 1369, 2879)/6	(371, 770, 1371)/4
	$F6$	(6558, 31329, 55924)/3430	(5172, 15713, 41423)/4022	(3622, 8377, 20615)/1562	(2438, 6545, 16439)/2135

Table C.3. Number of scenarios required for different O-D pairs under $F2$.

No.	O-D pair	$RD \leq 1\%$ RS/SG	$RD \leq 2\%$ RS/SG	$RD \leq 5\%$ RS/SG
1	(65, 35)	70/10	45/10	15/10
2	(19, 150)	45/10	25/10	10/10
3	(16, 29)	90/10	45/10	10/10
4	(16, 26)	85/10	50/10	20/10
5	(38, 15)	98/10	75/10	45/10
6	(37, 66)	90/10	60/10	25/10
7	(41, 82)	90/15	65/10	25/10
8	(152, 85)	95/10	65/10	20/10
9	(22, 42)	90/10	45/10	10/10
10	(57, 6)	90/15	55/10	25/10
11	(84, 119)	98/15	85/10	45/10
12	(36, 72)	98/10	55/10	15/10

Table C.4. Number of scenarios required for different O-D pairs under $F3$.

No.	O-D pair	$RD \leq 1\%$ RS/SG	$RD \leq 2\%$ RS/SG	$RD \leq 5\%$ RS/SG
1	(65, 35)	80/10	45/10	15/10
2	(19, 150)	65/10	25/10	10/10
3	(16, 29)	70/10	40/10	10/10
4	(16, 26)	75/10	35/10	10/10
5	(38, 15)	98/10	98/10	25/10
6	(37, 66)	98/10	98/10	15/10
7	(41, 82)	80/10	50/10	15/10
8	(152, 85)	75/10	50/10	15/10
9	(22, 42)	98/10	98/10	10/10
10	(57, 6)	98/10	98/10	20/10
11	(84, 119)	85/15	55/10	20/10
12	(36, 72)	70/10	30/10	10/10

Appendix D. Detailed results of O-D pair (65, 35) in the freeway network

In Section 4.4, we use O-D pair (65, 35) as an example to describe the effects of different parameters in the objective functions on RD, VAR, and ORD results. The detailed results of O-D pair (65, 35) under different objective functions are shown in this appendix. Tables D.1, D.3, D.5 and D.7 show the RD and VAR results at different S for objective functions $F1$, $F4$, $F5$ and $F6$, respectively. The format of these tables is the same with the format of Tables C.1 and C.2. Tables D.2, D.4, D.6, and D.8 show the ORD results for objective functions $F1$, $F4$, $F5$ and $F6$, respectively. In these tables, the values separated by a slash in each cell represent the results generated by RS and SG, respectively.

To further clarify Point 2 in Section 4.4, we give some detailed analyses for it as follows.

1. When the objective is some kind of expectation of travel time (i.e., approximates the expected travel time $F2$), the variation represented by RD and VAR is relatively small. As shown in the tables of RD and VAR results, $F1$ with small θ, $F4$ with small D, $F5$ with small time interval $D - E$, and $F6$ with a specific α (e.g., $\alpha = 0.3$) could result in relatively small RDs and VARs on the whole. The reason is simple. Given a path, the expectation of its travel times or carbon emissions in S scenarios generally have small difference for $2m + 1$ scenario sets, especially in the scenario sets generated by SG, where the mean of travel speeds on each link and each path is controlled to be equal to the mean of the given distribution.
2. When the objective function does not approximate the objective $F2$, both methods, but particularly the RS method, will be very sensitive to what happens to be the extreme values in a scenario set. As shown in the tables of RD and VAR results, on the whole, large RDs and VARs are produced for $F1$ with large θ, $F4$ with large D, $F5$ with large time interval $D - E$, and $F6$ with relatively small or large α. Taking $F4$ with $D = 9.00$ and $S = 10$ as an example, the objective value of a path is equal to the mean of the tardiness $\max(D_p + T^s - D, 0)$ in 10 scenarios. In this case, the tardiness values in most scenarios are 0. The non-zero tardiness values, especially very large values from some extreme scenarios, have large effects on the value of $F4$. Then, even if we use SG to generate scenarios, the optimal objective values in $2m + 1$ scenario sets would vary a lot, which results in large RDs and VARs as shown in Table D.3. Even so, SG always generates smaller RDs and VARs than RS does.

Table D.1. Comparison of RD and VAR as generated by RS and SG for O-D pair (65, 35) and different θ in $F1$.

	θ	$S = 10$ RS/SG	$S = 15$ RS/SG	$S = 20$ RS/SG	$S = 25$ RS/SG
	0	(3.42, 5.60, 7.65)/0.44	(2.6, 4.01, 6.67)/0.12	(2.35, 3.12, 3.79)/0.23	(1.60, 3.21, 5.84)/0.18
	0.2	(3.62, 6.28, 9.25)/0.37	(2.74, 4.56, 6.50)/0.23	(2.54, 3.24, 3.92)/0.28	(1.77, 2.52, 4.06)/0.30
	0.4	(3.99, 7.18, 10.55)/0.35	(2.68, 4.62, 6.47)/0.33	(2.94, 3.60, 5.06)/0.33	(2.13, 3.14, 4.58)/0.42
	0.6	(5.49, 7.49, 9.96)/0.37	(3.16, 4.62, 5.97)/0.44	(2.55, 3.61, 4.98)/0.38	(1.82, 3.38, 6.20)/0.54
	0.8	(6.22, 7.64, 10.64)/0.49	(3.93, 5.36, 12.21)/0.54	(2.60, 4.55, 6.85)/0.45	(2.52, 3.61, 6.60)/0.68
$RD(\%)$	1.0	(4.52, 7.70, 11.64)/0.60	(2.51, 6.00, 11.11)/0.64	(2.44, 4.30, 5.75)/0.52	(2.26, 3.56, 5.49)/0.81
	1.2	(6.76, 8.96, 14.13)/0.70	(4.35, 6.35, 9.45)/0.74	(2.56, 4.56, 6.61)/0.59	(2.40, 3.70, 4.79)/0.94
	1.4	(4.02, 9.60, 14.57)/0.81	(4.45, 6.39, 9.18)/0.85	(4.69, 6.01, 8.02)/0.66	(2.74, 4.40, 6.09)/1.07
	1.6	(6.00, 10.47, 15.21)/1.10	(4.92, 7.38, 10.09)/1.12	(4.23, 5.44, 7.42)/0.86	(3.12, 4.75, 6.61)/1.19
	1.8	(5.27, 11.20, 16.89)/1.21	(3.77, 6.66, 13.21)/1.23	(4.30, 7.75, 12.00)/0.95	(3.56, 5.37, 7.10)/1.32
	2.0	(5.94, 11.49, 17.39)/1.32	(5.29, 8.80, 14.16)/1.34	(5.54, 7.13, 8.19)/1.03	(4.06, 5.05, 6.57)/1.44
	0	(1729, 3945, 8040)/16	(822, 2263, 6260)/2	(775, 1081, 1430)/6	(299, 1412, 4441)/4
	0.2	(1629, 4892, 9596)/14	(758, 2744, 5883)/7	(676, 1310, 2288)/9	(350, 809, 1672)/10
	0.4	(2045, 6289, 11614)/16	(994, 3131, 5906)/15	(1131, 1590, 3063)/13	(688, 1279, 2294)/20
	0.6	(4058, 7606, 11472)/22	(1334, 2870, 4753)/26	(912, 1781, 2561)/19	(309, 1527, 4478)/36
	0.8	(5022, 9199, 18491)/32	(1741, 4276, 18287)/42	(967, 3140, 7607)/27	(745, 2382, 10465)/56
VAR	1.0	(2356, 8720, 19638)/46	(953, 6065, 18310)/60	(741, 2258, 3339)/35	(601, 1908, 4068)/81
	1.2	(4653, 10649, 29516)/63	(2527, 5918, 12948)/82	(924, 3416, 6010)/46	(684, 1915, 3017)/110
	1.4	(2607, 14013, 31953)/85	(2695, 6355, 15095)/108	(2842, 4787, 8139)/57	(1172, 2996, 4385)/144
	1.6	(4424, 19466, 39131)/200	(3185, 8294, 19264)/161	(2136, 4227, 7570)/82	(1305, 3462, 6783)/183
	1.8	(4140, 21958, 43436)/251	(2318, 8249, 31277)/196	(2785, 9215, 19187)/99	(1566, 4692, 8950)/227
	2.0	(5939, 23145, 46295)/309	(4783, 13340, 34110)/235	(5807, 7419, 10353)/118	(2376, 4046, 6920)/275

Table D.2. $ORD(\%)$ values as generated by RS and SG for O-D pair (65, 35) and different θ in $F1$.

θ	$S = 10$ RS/SG	$S = 15$ RS/SG	$S = 20$ RS/SG	$S = 25$ RS/SG
0	0.25/0	0.07/0	0.02/0	0.07/0
0.2	0.25/0	0.17/0	0.08/0	0.06/0
0.4	0.39/0	0.23/0	0.09/0	0.04/0
0.6	0.42/0	0.13/0	0.11/0	0.15/0
0.8	0.51/0	0.31/0	0.27/0	0.14/0
1.0	0.72/0	0.42/0	0.25/0	0.13/0
1.2	0.69/0	0.36/0	0.28/0	0.15/0
1.4	0.54/0	0.43/0	0.40/0	0.17/0
1.6	0.88/0.02	0.52/0.02	0.24/0.05	0.26/0.05
1.8	0.79/0.04	0.47/0.06	0.58/0.08	0.23/0.08
2.0	0.78/0.04	0.45/0.04	0.46/0.05	0.32/0.05

Table D.3. Comparison of RD and VAR as generated by RS and SG for O-D pair (65, 35) and different D in $F4$.

	D	$S = 10$ RS/SG	$S = 15$ RS/SG	$S = 20$ RS/SG	$S = 25$ RS/SG
$RD(\%)$	8.86	(28.37, 38.32, 51.23)/4.03	(19.58, 26.75, 36.75)/1.13	(14.96, 22.26, 31.56)/2.05	(15.40, 22.86, 29.92)/1.65
	8.88	(22.38, 41.65, 57.92)/4.96	(32.16, 39.06, 45.63)/1.40	(16.96, 31.18, 45.24)/2.52	(17.62, 25.48, 30.48)/2.03
	8.90	(48.88, 54.16, 62.50)/4.54	(16.53, 38.84, 60.79)/3.21	(23.85, 34.95, 43.25)/4.44	(16.08, 26.95, 37.95)/3.72
	8.92	(58.72, 64.70, 72.90)/7.58	(39.35, 47.69, 56.44)/3.71	(24.84, 37.69, 50.07)/4.56	(27.75, 40.52, 50.22)/5.78
	8.94	(58.75, 72.57, 86.25)/9.37	(38.90, 58.85, 74.62)/9.93	(32.67, 48.32, 82.56)/6.03	(32.7, 46.87, 66.27)/7.76
	8.96	(66.33, 82.42, 100)/10.05	(50.18, 68.31, 89.49)/14.68	(49.43, 61.14, 77.11)/7.48	(44.38, 54.41, 64.62)/12.67
	8.98	(64.16, 92.08, 100)/29.57	(76.93, 83.69, 100)/32.94	(55.95, 77.96, 97.51)/24.26	(50.11, 67.92, 86.36)/23.12
	9.00	(94.06, 99.41, 100)/44.18	(77.57, 90.42, 100)/47.88	(68.28, 84.85, 99.61)/47.88	(55.19, 75.86, 95.56)/42.20
VAR	8.86	(1804, 4728, 9161)/16	(808, 1526, 2966)/2	(441, 997, 2237)/6	(337, 959, 1446)/4
	8.88	(767, 4505, 10135)/16	(1128, 2376, 3986)/2	(486, 1392, 2411)/6	(332, 802, 1035)/4
	8.90	(2764, 4176, 6071)/10	(205, 1742, 4027)/6	(439, 1165, 2023)/10	(217, 595, 983)/6
	8.92	(1630, 4762, 7981)/13	(698, 1276, 2120)/5	(374, 817, 1544)/6	(407, 908, 1478)/9
	8.94	(1033, 3771, 7302)/11	(247, 1496, 3135)/16	(283, 1278, 6537)/5	(191, 598, 1188)/9
	8.96	(784, 2252, 4859)/10	(316, 1263, 3017)/16	(282, 759, 1530)/4	(250, 475, 824)/9
	8.98	(290, 3034, 6625)/17	(270, 704, 1284)/30	(153, 558, 1874)/10	(138, 377, 837)/12
	9.00	(767, 1799, 4422)/17	(79, 794, 2744)/17	(203, 433, 1305)/16	(63, 251, 1020)/16

Table D.4. $ORD(\%)$ values as generated by RS and SG for O-D pair (65, 35) and different D in $F4$.

D	$S = 10$ RS/SG	$S = 15$ RS/SG	$S = 20$ RS/SG	$S = 25$ RS/SG
8.86	3.67/0	1.24/0	0.07/0	0.10/0
8.88	2.77/0	0.91/0	0.17/0	0.33/0
8.90	3.05/0	1.14/0	0.10/0	0.20/0
8.92	5.26/0	1.41/0	0.58/0	0.69/0
8.94	11.78/0	3.52/0	2.02/0	0.74/0
8.96	13.08/0	7.25/0	4.94/0	1.56/0
8.98	24.12/0	8.40/0	7.17/0	5.37/0
9.00	23.60/1.04	14.68/2.08	11.19/4.15	7.52/4.15

Table D.5. Comparison of RD and VAR as generated by RS and SG for O-D pair (65, 35) and different time windows in $F5$.

	Time window	$S = 10$ RS/SG	$S = 15$ RS/SG	$S = 20$ RS/SG	$S = 25$ RS/SG
$RD(\%)$	(8.90, 8.93)	(48.17, 63.28, 82.01)/6.93	(38.22, 49.31, 65.83)/6.93	(31.79, 47.31, 59.09)/5.82	(27.51, 40.09, 49.81)/8.06
	(8.87, 8.96)	(69.55, 77.71, 95.98)/10.05	(55.18, 71.28, 86.17)/14.68	(52.44, 60.92, 68.19)/7.48	(45.51, 57.32, 75.74)/12.67
	(8.84, 8.99)	(85.21, 97.69, 100)/31.66	(76.77, 86.73, 100)/38.07	(67.15, 80.45, 96.81)/36.95	(56.55, 74.08, 93.31)/32.26
	(8.84, 8.93)	(50.23, 65.09, 92.09)/7.13	(26.71, 44.01, 63.85)/5.18	(30.49, 45.69, 52.91)/4.99	(30.97, 39.66, 48.60)/6.48
	(8.81, 8.90)	(42.61, 53.20, 63.03)/4.54	(24.33, 44.11, 67.52)/3.21	(31.15, 38.53, 43.61)/4.44	(24.58, 29.63, 37.58)/3.72
	(8.78, 8.87)	(22.64, 40.01, 50.80)/4.45	(24.83, 32.00, 41.12)/1.25	(21.74, 27.33, 30.67)/2.26	(15.52, 24.02, 30.30)/1.82
	(8.9, 8.99)	(84.19, 94.02, 100)/33.05	(69.94, 83.11, 97.86)/40.25	(70.17, 82.82, 95.02)/39.22	(62.64, 70.51, 83.02)/34.06
	(8.93, 9.02)	(88.43, 96.38, 100)/57.60	(80.81, 87.27, 95.68)/54.06	(79.64, 84.16, 91.44)/49.03	(57.54, 73.68, 86.1)/44.31
	(8.96, 9.05)	(96.17, 99.59, 100)/69.02	(84.34, 93.54, 98.87)/41.07	(82.76, 92.66, 99.74)/40.95	(70.27, 82.29, 98.70)/50.47
VAR	(8.90, 8.93)	(823, 3035, 9092)/10	(589, 1091, 2089)/15	(333, 1005, 1493)/8	(285, 709, 1124)/11
	(8.87, 8.96)	(715, 1546, 3218)/10	(435, 1169, 1987)/16	(452, 918, 3604)/4	(220, 464, 1045)/9
	(8.84, 8.99)	(739, 1545, 3607)/14	(346, 566, 1151)/27	(186, 667, 3046)/20	(136, 275, 477)/15
	(8.84, 8.93)	(880, 2371, 4783)/9	(218, 1302, 5976)/7	(407, 1037, 2809)/4	(275, 535, 888)/8
	(8.81, 8.90)	(2678, 4448, 7732)/10	(590, 1806, 3897)/6	(703, 1369, 2879)/10	(371, 770, 1371)/6
	(8.78, 8.87)	(764, 3554, 6803)/16	(777, 1832, 2694)/2	(611, 1188, 1634)/6	(376, 858, 1334)/4
	(8.90, 8.99)	(303, 1458, 2814)/20	(209, 696, 1971)/32	(135, 478, 804)/21	(171, 338, 1041)/18
	(8.93, 9.02)	(652, 1475, 2536)/42	(357, 752, 1424)/33	(195, 631, 1070)/28	(73, 355, 780)/21
	(8.96, 9.05)	(411, 1402, 4678)/57	(434, 751, 1623)/29	(147, 426, 1053)/25	(177, 296, 845)/48

Table D.6. $ORD(\%)$ values as generated by RS and SG for O-D pair (65, 35) and different time windows in $F5$.

Time window	$S = 10$ RS/SG	$S = 15$ RS/SG	$S = 20$ RS/SG	$S = 25$ RS/SG
(8.90, 8.93)	3.95/0	3.31/0	1.57/0	1.87/0
(8.87, 8.96)	6.26/0	6.28/0	3.97/0	1.99/0
(8.84, 8.99)	19.19/1.58	8.85/1.58	9.55/1.58	7.40/1.58
(8.84, 8.93)	4.22/0	2.04/0	1.41/0	1.37/0
(8.81, 8.90)	4.37/0	1.09/0	0.50/0	0.10/0
(8.78, 8.87)	1.59/0	1.26/0	0.52/0	0.15/0
(8.90, 8.99)	18.33/2.94	9.96/1.96	7.58/1.96	8.22/3.92
(8.93, 9.02)	31.92/8.62	22.29/2.87	26.33/2.87	16.5/4.91
(8.96, 9.05)	19.03/4.01	20.48/14.24	16.29/13.17	13.07/11.69

Table D.7. Comparison of RD and VAR as generated by RS and SG for O-D pair (65, 35) and different α in $F6$.

	α	$S = 10$ RS/SG	$S = 15$ RS/SG	$S = 20$ RS/SG	$S = 25$ RS/SG
$RD(\%)$	0.1	(3.77, 7.93, 11.14)/4.17	(4.84, 6.41, 8.74)/3.26	(2.72, 4.98, 7.14)/3.01	(3.28, 4.26, 5.31)/1.58
	0.2	(5.67, 7.29, 10.89)/5.67	(4.81, 5.81, 6.78)/3.25	(4.03, 4.93, 6.84)/3.29	(3.66, 4.48, 5.94)/3.80
	0.3	(4.79, 6.87, 8.65)/3.45	(4.27, 5.82, 7.50)/3.80	(3.45, 4.64, 6.54)/3.80	(2.65, 3.90, 5.29)/2.14
	0.4	(5.52, 7.14, 10.35)/5.43	(3.70, 5.55, 8.00)/4.29	(3.31, 4.41, 5.33)/3.80	(3.33, 4.21, 5.68)/2.09
	0.5	(5.15, 8.28, 10.41)/5.30	(1.89, 5.55, 10.07)/4.62	(3.31, 5.39, 7.55)/1.10	(2.11, 3.56, 5.29)/2.44
	0.6	(5.54, 8.74, 11.86)/2.48	(3.61, 5.64, 7.96)/2.47	(2.91, 3.65, 5.12)/2.09	(2.46, 3.68, 5.47)/2.22
	0.7	(5.09, 8.85, 14.22)/3.61	(5.32, 6.49, 8.56)/3.14	(2.28, 4.58, 7.30)/2.48	(2.07, 4.23, 6.36)/2.02
	0.8	(7.66, 10.51, 14.45)/3.44	(5.28, 7.06, 9.05)/2.40	(3.91, 5.95, 7.73)/2.22	(3.27, 5.01, 7.44)/2.62
	0.9	(7.09, 13.25, 18.62)/4.67	(6.33, 8.88, 14.13)/4.88	(6.02, 7.31, 11.62)/3.87	(4.66, 6.35, 8.43)/4.33
	1.0	(9.52, 14.51, 18.62)/3.13	(3.71, 9.96, 17.08)/2.65	(8.67, 10.99, 12.86)/4.70	(7.13, 11.07, 15.16)/4.59
VAR	0.1	(2528, 6938, 14311)/1500	(2428, 4616, 8732)/1030	(766, 2801, 5351)/946	(1146, 2164, 3939)/293
	0.2	(3785, 6767, 11297)/4967	(2912, 3902, 6002)/989	(1750, 3169, 8657)/1017	(1211, 2380, 3966)/1188
	0.3	(2636, 5744, 12385)/1511	(1719, 3871, 6902)/1889	(1359, 2879, 3748)/1968	(1115, 1955, 3241)/377
	0.4	(3757, 5915, 9535)/3200	(1044, 3571, 6408)/1803	(1154, 2659, 4464)/1142	(1066, 1999, 4406)/344
	0.5	(2381, 7998, 12812)/3475	(315, 3962, 9092)/2071	(1324, 3522, 7207)/128	(582, 1780, 4640)/802
	0.6	(5763, 9744, 16466)/797	(1435, 4511, 7469)/766	(855, 1653, 3984)/573	(736, 1663, 3199)/541
	0.7	(3171, 10853, 27934)/1548	(3073, 5213, 8311)/1049	(668, 3173, 6593)/646	(469, 2473, 4362)/613
	0.8	(10611, 18373, 38065)/1838	(4382, 7845, 12156)/818	(2303, 5802, 9212)/713	(1925, 4068, 8083)/917
	0.9	(6558, 31329, 55924)/3430	(5172, 15713, 41423)/4022	(3622, 8377, 20615)/1562	(2438, 6545, 16439)/2135
	1.0	(20687, 43022, 61234)/1579	(3652, 17016, 39717)/900	(16007, 26113, 38528)/2910	(11292, 25954, 44208)/2179

Table D.8. $ORD(\%)$ values as generated by RS and SG for O-D pair (65, 35) and different α in $F6$.

α	$S = 10$ RS/SG	$S = 15$ RS/SG	$S = 20$ RS/SG	$S = 25$ RS/SG
0.1	0.55/0.80	0.41/0.80	0.39/0.53	0.39/0.28
0.2	0.50/0.64	0.53/0.31	0.45/0.17	0.37/0.17
0.3	0.32/0.02	0.24/0.21	0.19/0.21	0.20/0.02
0.4	0.59/0.79	0.36/0.46	0.25/0.17	0.45/0.05
0.5	0.50/0.44	0.27/0.29	0.36/0	0.17/0.15
0.6	0.68/0.18	0.35/0.28	0.21/0.18	0.16/0
0.7	0.70/0.66	0.27/0.21	0.24/0.11	0.24/0.05
0.8	0.79/0.31	0.53/0.06	0.31/0.04	0.30/0.02
0.9	0.86/0.53	0.53/0.38	0.44/0.23	0.37/0.25
1.0	3.91/2.45	2.43/0.73	2.12/1.22	2.25/1.90

Appendix E. Results in an urban road network

To test the RS and SG methods for urban road networks, we further conduct experiments in a road network of Chengdu city in western China. The underlying road network, as shown in Fig. E.1, includes 408 nodes and 1,250 road links within the first ring of Chengdu. We consider 30 2-min time periods between 3pm and 4pm, which leads to 37,500 (1250 links $\times$30 periods) random speed variables. It is more than three times the 10,512 random speed variables in the California freeway network, which is approximately the largest problem size that can be handled by our laptop with 16GB RAM used for this research. We use the 110-day real speed dataset described in Guo et al. (2020). We test the two methods for 10 O-D pairs and $S = 10, 20, 30, 40$ under the same six objective functions described in Section 4.3.

Tables E.1 and E.2 present the RD, VAR and ORD results for 10 different O-D pairs under objective function $F1$. To be consistent with the tables above, we present the minimum, the mean, the maximum of RDs and VARs, and the mean of ORDs in ten runs for RS in the tables. The results support the finding from the freeway network that, for all O-D pairs, SG generates much smaller RDs and VARs than RS does, and SG achieves much smaller ORDs with only 10 scenarios. However, compared with the RDs and VARs of the freeway network in Table B.1 and the ORDs in Table 2, we find that the urban road network has much larger RDs, VARs and ORDs. Moreover, for SG, 40 scenarios ($S = 40$) cannot get a stability level of $RD \leq 5\%$ for all O-D pairs. That is, compared with freeway networks, we need more scenarios to achieve the same stability level in urban road networks. This result may be explained by the fact that urban road networks have a more complicated network topology, shorter road links, and higher speed variance. They are thus characterized by higher correlations of travel speeds in both space and time. This affects the number of scenarios required for the SSPs in urban road networks, but not the superiority of SG over RS.

Tables E.3 and E.4 present comparison results for O-D pair (22,128) under six different objective functions. We set the departure time D_p to 3pm, θ to 1.27 in $F1$, due time D to 15.10 (i.e., 15:6:00 in HH:MM:SS format) in $F4$, time window (E, D) to (15.09,15.10) in $F5$, and on-time arrival probability α to 60% in $F6$. It is obvious that, for the same O-D pair, different objective functions have large effects on the RDs, VARs and ORDs, but SG still outperforms RS in terms of the three metrics. Objective functions $F2$ and $F3$ lead to much smaller RDs and VARs than objective functions $F4$ and $F5$ that consider earliness and / or tardiness do. These findings are consistent with those in the California freeway network.

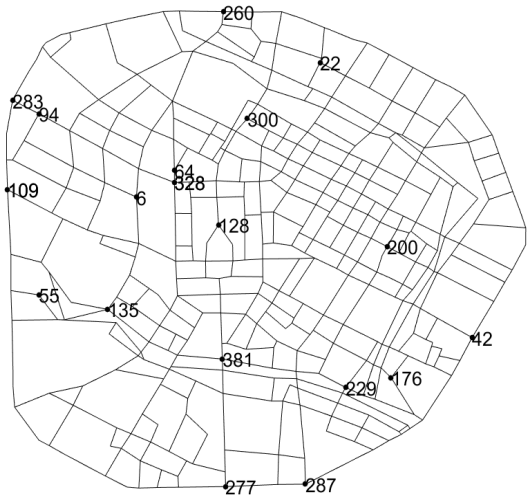

Fig. E.1. The Chengdu network within the first ring. The numbers refer to nodes that we use in the main text.

Table E.1. Comparison of RD and VAR as generated by RS and SG for different O-D pairs in the Chengdu road network.

	No.	O-D pair	$S = 10$ RS/SG	$S = 20$ RS/SG	$S = 30$ RS/SG	$S = 40$ RS/SG
RD(%)	1	(22,128)	(17.12,19.68,23.82)/8.60	(12.26,14.34,18.76)/8.06	(6.70,9.81,14.16)/4.91	(4.17,7.39,9.28)/3.47
	2	(287,260)	(11.96,16.04,20.40)/9.23	(5.30,8.90,12.09)/4.97	(4.05,7.52,10.90)/3.41	(2.54,4.71,7.08)/3.98
	3	(55,64)	(13.53,20.21,26.53)/10.28	(5.21,15.05,21.39)/5.87	(5.56,9.06,18.15)/3.30	(4.88,7.64,9.93)/2.52
	4	(6,300)	(15.23,22.04,27.50)/10.06	(7.33,14.67,17.24)/8.05	(5.14,10.83,13.85)/7.90	(6.85,9.74,14.13)/6.47
	5	(176,200)	(21.81,28.50,34.14)/11.23	(12.82,17.44,22.45)/7.69	(6.43,11.84,15.25)/4.06	(6.80,10.18,14.46)/4.05
	6	(109,42)	(6.91,13.68,18.28)/7.87	(6.24,11.06,15.98)/3.85	(6.81,7.83,9.54)/4.70	(3.33,5.65,8.16)/4.97
	7	(229,135)	(21.84,27.43,34.36)/15.20	(13.49,18.28,23.29)/10.28	(9.22,13.56,18.79)/7.60	(8.84,11.76,16.26)/7.28
	8	(94,328)	(13.11,23.35,31.82)/5.46	(13.19,18.10,25.13)/5.66	(11.98,14.86,18.73)/5.92	(8.89,11.34,17.30)/4.76
	9	(283,328)	(12.56,20.16,27.59)/9.82	(8.13,13.77,18.54)/6.58	(7.90,12.35,16.22)/5.36	(7.51,9.32,11.17)/4.64
	10	(277,381)	(11.89,22.07,30.43)/7.62	(9.39,14.12,19.46)/4.37	(8.71,13.53,17.94)/4.32	(7.09,10.25,14.00)/3.36
VAR	1	(22,128)	(807,1238,1894)/167	(330,582,985)/147	(138,259,461)/57	(62,154,211)/43
	2	(287,260)	(1303,2910,4573)/765	(439,826,1358)/167	(166,568,1028)/125	(79,262,660)/140
	3	(55,64)	(564,2041,3570)/300	(79,1067,2129)/159	(92,335,1380)/46	(73,197,370)/21
	4	(6,300)	(225,725,1535)/91	(66,295,485)/51	(37,164,340)/54	(64,117,174)/55
	5	(176,200)	(718,1246,1826)/119	(190,419,740)/92	(55,195,296)/18	(55,126,202)/18
	6	(109,42)	(482,1902,3292)/355	(344,1145,2628)/117	(329,578,849)/146	(110,329,731)/192
	7	(229,135)	(2174,3449,5675)/650	(692,1249,1860)/282	(359,715,1565)/116	(277,475,747)/137
	8	(94,328)	(144,603,926)/28	(194,344,740)/18	(117,212,332)/23	(73,111,213)/11
	9	(283,328)	(294,755,1460)/113	(104,285,443)/43	(80,205,352)/39	(87,113,165)/21
	10	(277,381)	(118,549,1100)/36	(65,195,345)/18	(82,173,328)/16	(43,92,193)/8

Table E.2. $ORD(\%)$ values at different S generated by RS and SG for different O-D pairs in the Chengdu road network.

No.	O-D pair	$S=10$ RS/SG	$S=20$ RS/SG	$S=30$ RS/SG	$S=40$ RS/SG
1	(22,128)	2.63/0.95	1.99/0.84	1.19/0.95	0.57/0
2	(287,260)	2.55/0.96	1.18/0.70	0.87/0.50	0.32/0.50
3	(55,64)	1.87/0	0.94/0	0.14/0	0/0
4	(6,300)	2.72/1.44	1.15/1.44	0.29/0	0/0
5	(176,200)	5.02/0.41	2.78/0.41	1.38/0	0.69/0
6	(109,42)	0.72/0.30	0.09/0	0/0	0/0
7	(229,135)	4.81/1.86	2.51/0.56	1.52/0	0.89/0
8	(94,328)	1.16/0	0.42/0	0.11/0	0.11/0
9	(283,328)	1.16/0	0.45/0	0/0	0/0
10	(277,381)	0/0	0/0	0/0	0/0

Table E.3. Comparison of RD and VAR as generated by RS and SG for O-D pair (22,128) and different objective functions in the Chengdu road network.

	Objective function	$S=10$ RS/SG	$S=20$ RS/SG	$S=30$ RS/SG	$S=40$ RS/SG
$RD(\%)$	$F1$	(17.12,19.68,23.82)/8.60	(12.26,14.34,18.76)/8.06	(6.70,9.81,14.16)/4.91	(4.17,7.39,9.28)/3.47
	$F2$	(9.28,14.24,17.13)/2.84	(7.25,9.63,12.37)/2.98	(4.99,6.72,9.84)/1.27	(4.10,5.73,7.79)/1.33
	$F3$	(7.36,9.80,14.28)/2.15	(5.21,6.46,8.73)/1.19	(2.93,4.73,5.96)/0.83	(1.52,2.85,5.74)/0
	$F4$	(39.48,54.52,69.42)/16.60	(29.66,39.13,48.46)/18.16	(16.30,26.01,37.09)/6.95	(15.71,22.77,30.32)/9.22
	$F5$	(45.52,60.32,69.10)/17.87	(33.88,41.32,49.36)/19.16	(24.12,33.43,40.04)/7.03	(17.62,24.47,32.91)/10.86
	$F6$	(12.41,19.09,26.22)/8.31	(9.09,12.21,17.31)/7.52	(5.91,9.39,12.55)/5.93	(2.86,6.11,7.24)/5.15
VAR	$F1$	(807,1238,1894)/167	(330,582,985)/147	(138,259,461)/57	(62,154,211)/43
	$F2$	(184,428,764)/17	(95,193,296)/14	(56,85,184)/3	(37,63,94)/3
	$F3$	(0,0,0)/0	(0,0,0)/0	(0,0,0)/0	(0,0,0)/0
	$F4$	(263,437,776)/18	(94,165,247)/16	(20,69,151)/2	(18,50,84)/4
	$F5$	(295,409,608)/18	(90,184,294)/16	(67,96,132)/2	(21,44,86)/5
	$F6$	(389,917,1902)/169	(156,327,683)/120	(65,196,429)/72	(20,80,130)/56

Table E.4. $ORD(\%)$ values at different S generated by RS and SG for O-D pair (22,128) and different objective functions in the Chengdu road network.

Objective function	$S=10$ RS/SG	$S=20$ RS/SG	$S=30$ RS/SG	$S=40$ RS/SG
$F1$	2.63/0.95	1.99/0.84	1.19/0.95	0.57/0
$F2$	2.03/0.29	1.14/0	0.52/0	0.39/0
$F3$	0.63/0	0.27/0	0.12/0	0.02/0
$F4$	8.53/0	6.50/0	2.04/0	1.24/0
$F5$	7.43/0	5.53/0	2.69/0	0.95/0
$F6$	2.59/0.67	1.43/0.81	0.97/1.11	0.53/0.78

References

Akiba, T., Iwata, Y., Yoshida, Y., 2013. Fast exact shortest-path distance queries on large networks by pruned landmark labeling, in: Proceedings of the 2013 international conference on Management of data - SIGMOD '13, ACM Press, New York, New York, USA. p. 349. doi:10.1145/2463676.2465315.

Avraham, E., Raviv, T., 2020. The data-driven time-dependent traveling salesperson problem. Transportation Research Part B: Methodological 134, 25–40. doi:10.1016/j.trb.2020.01.005.

Bast, H., Delling, D., Goldberg, A., Müller-Hannemann, M., Pajor, T., Sanders, P., Wagner, D., Werneck, R.F., 2016. Route planning in transportation networks, in: Algorithm engineering. Springer, Cham, pp. 19–80. doi:10.1007/978-3-319-49487-6_2.

Brown, G.G., Carlyle, W.M., 2019. Solving the nearly symmetric all-pairs shortest-path problem. INFORMS Journal on Computing doi:10.1287/ijoc.2018.0873.

Chen, M., Mehrotra, S., Papp, D., 2015. Scenario generation for stochastic optimization problems via the sparse grid method. Computational Optimization and applications 62, 669–692.

Chen, P., Tong, R., Lu, G., Wang, Y., 2018. The alpha-reliable path problem in stochastic road networks with link correlations: A moment-matching-based path finding algorithm. Expert Systems with Applications 110, 20–32. doi:10.1016/j.eswa.2018.05.022.

Cheng, T., Haworth, J., Wang, J., 2012. Spatio-temporal autocorrelation of road network data. Journal of Geographical Systems 14, 389–413. doi:10.1007/s10109-011-0149-5.

Deo, N., Pang, C.Y., 1984. Shortest-path algorithms: Taxonomy and annotation. Networks 14, 275–323. doi:10.1002/net.3230140208.

Ehmke, J.F., Campbell, A.M., Thomas, B.W., 2016. Data-driven approaches for emissions-minimized paths in urban areas. Computers & Operations Research 67, 34–47. doi:10.1016/j.cor.2015.08.013.

Gao, S., 2005. Optimal adaptive routing and traffic assignment in stochastic time-dependent networks. Ph.D. thesis. Massachusetts Institute of Technology.

Gendreau, M., Ghiani, G., Guerriero, E., 2015. Time-dependent routing problems: A review. Computers & Operations Research 64, 189–197. doi:10.1016/j.cor.2015.06.001.

Gu, Y., Wallace, S.W., Wang, X., 2019. Integrated maritime fuel management with stochastic fuel prices and new emission regulations. Journal of the Operational Research Society 70, 707–725. doi:10.1080/01605682.2017.1415649.

Guo, F., Gu, X., Guo, Z., Dong, Y., Wallace, S.W., 2020. Understanding the marginal distributions and correlations of link travel speeds in road networks. Scientific reports 10, 1–8. doi:10.1038/s41598-020-68810-9.

Guo, F., Zhang, D., Dong, Y., Guo, Z., 2019a. Urban link travel speed dataset from a megacity road network. Scientific Data 6, 61. doi:10.1038/s41597-019-0060-3.

Guo, Z., Wallace, S.W., Kaut, M., 2019b. Vehicle routing with space- and time-correlated stochastic travel times: Evaluating the objective function. INFORMS Journal on Computing 31, 654–670. doi:10.1287/ijoc.2019.0906.

Hall, R.W., 1986. The fastest path through a network with random time-dependent travel times. Transportation Science 20, 182–188. doi:10.1287/trsc.20.3.182.

Hickman, J., Hassel, D., Joumard, R., Samaras, Z., Sorenson, S., 1999. MEET-methodology for calculating transport emissions and energy consumption. Technical Report. European Commission, DG VII.

Holtz, M., 2010. Sparse grid quadrature in high dimensions with applications in finance and insurance. volume 77. Springer Science & Business Media.

Høyland, K., Kaut, M., Wallace, S.W., 2003. A heuristic for moment-matching scenario generation. Computational optimization and applications 24, 169–185.

Hu, H., Sotirov, R., 2019. On solving the quadratic shortest path problem. INFORMS Journal on Computing 32, 219–233. doi:10.1287/ijoc.2018.0861.

Hu, J., Yang, B., Guo, C., Jensen, C.S., 2018. Risk-aware path selection with time-varying, uncertain travel costs: a time series approach. The VLDB Journal 27, 179–200. doi:10.1007/s00778-018-0494-9.

Huang, H., Gao, S., 2012. Optimal paths in dynamic networks with dependent random link travel times. Transportation Research Part B: Methodological 46, 579–598. doi:10.1016/j.trb.2012.01.005.

Huang, H., Gao, S., 2018. Trajectory-adaptive routing in dynamic networks with dependent random link travel times. Transportation Science 52, 102–117. doi:10.1287/trsc.2016.0691.

Kaut, M., 2014. A copula-based heuristic for scenario generation. Computational Management Science 11, 503–516. doi:10.1007/s10287-014-0224-8.

Kaut, M., Wallace, S.W., 2007. Evaluation of scenario-generation methods for stochastic programming. Pacific Journal of Optimization 3, 257–271. doi:10.18452/8296.

Krioukov, D., Fall, K., Yang, X., 2004. Compact routing on Internet-like graphs, in: IEEE Annual Joint Conference: INFOCOM, IEEE Computer and Communications Societies, IEEE, Hong Kong, China. pp. 209–219. doi:10.1109/INFCOM.2004.1354495.

Köster, F., Ulmer, M.W., Mattfeld, D.C., Hasle, G., 2018. Anticipating emission-sensitive traffic management strategies for dynamic delivery routing. Transportation Research Part D: Transport and Environment 62, 345–361. doi:10.1016/j.trd.2018.03.002.

Löhndorf, N., 2016. An empirical analysis of scenario generation methods for stochastic optimization. European Journal of Operational Research 255, 121–132. URL: http://www.sciencedirect.com/science/article/pii/S0377221716303411, doi:https://doi.org/10.1016/j.ejor.2016.05.021.

Mahmassani, H.S., Sbayti, H., 2009. DYNASMART-P Version 1.6 User's Guide. Northwestern University Transportation Center. Evanston.

Maiorino, E., Baek, S.H., Guo, F., Zhou, X., Kothari, P.H., Silverman, E.K., Barabási, A.L., Weiss, S.T., Raby, B.A., Sharma, A., 2020. Discovering the genes mediating the interactions between chronic respiratory diseases in the human interactome. Nature Communications 11, 811. doi:10.1038/s41467-020-14600-w.

Homem-de Mello, T., Bayraksan, G., 2014. Monte carlo sampling-based methods for stochastic optimization. Surveys in Operations Research and Management Science 19, 56–85. doi:10.1016/j.sorms.2014.05.001.

Miller-Hooks, E.D., Mahmassani, H.S., 2000. Least expected time paths in stochastic, time-varying transportation networks. Transportation Science 34, 198–215. doi:10.2307/25768909.

Noland, R.B., Small, K.A., Koskenoja, P.M., Chu, X., 1998. Simulating travel reliability. Regional Science and Urban Economics 28, 535–564. doi:10.1016/S0166-0462(98)00009-X.

Pedersen, S.A., Yang, B., Jensen, C.S., 2020. Fast stochastic routing under time-varying uncertainty. The VLDB Journal 29, 819–839. doi:10.1007/s00778-019-00585-6.

Pflug, G.C., 2001. Scenario tree generation for multiperiod financial optimization by optimal discretization. Mathematical programming 89, 251–271.

Prakash, A.A., 2018. Pruning algorithm for the least expected travel time path on stochastic and time-dependent networks. Transportation Research Part B: Methodological 108, 127–147. doi:10.1016/j.trb.2017.12.015.

Prakash, A.A., Srinivasan, K.K., 2018. Pruning algorithms to determine reliable paths on networks with random and correlated link travel times. Transportation Science 52, 80–101. doi:10.1287/trsc.2015.0668.

Rachtan, P., Huang, H., Gao, S., 2013. Spatiotemporal link speed correlations: Empirical study. Transportation Research Record: Journal of the Transportation Research Board 2390, 34–43. doi:10.3141/2390-04.

Shavitt, Y., Tankel, T., 2008. Hyperbolic embedding of Internet graph for distance estimation and overlay construction. IEEE/ACM Transactions on Networking 16, 25–36. doi:10.1109/TNET.2007.899021.

Sklar, A., 1973. Random variables, joint distribution functions, and copulas. Kybernetika 9, 449–460. URL: http://eudml.org/doc/28992.

Sommer, C., 2014. Shortest-path queries in static networks. ACM Computing Surveys 46, 1–31. doi:10.1145/2530531.

Wang, S., Wallace, S.W., Lu, J., Gu, Y., 2020. Handling financial risks in crude oil imports: Taking into account crude oil prices as well as country and transportation risks. Transportation Research Part E: Logistics and Transportation Review 133, 101824. doi:10.1016/j.tre.2019.101824.

Wang, X., Tan, K.S., 2013. Pricing and hedging with discontinuous functions: Quasi–monte carlo methods and dimension reduction. Management Science 59, 376–389.

Yang, B., Dai, J., Guo, C., Jensen, C.S., Hu, J., 2018. PACE: a PAth-CEntric paradigm for stochastic path finding. The VLDB Journal 27, 153–178. doi:10.1007/s00778-017-0491-4.

Yang, L., Zhou, X., 2014. Constraint reformulation and a lagrangian relaxation-based solution algorithm for a least expected time path problem. Transportation Research Part B: Methodological 59, 22–44. doi:10.1016/j.trb.2013.10.012.

Yang, L., Zhou, X., 2017. Optimizing on-time arrival probability and percentile travel time for elementary path finding in time-dependent transportation networks: Linear mixed integer programming reformulations. Transportation Research Part B: Methodological 96, 68–91. doi:10.1016/j.trb.2016.11.012.

Yen, J.Y., 1971. Finding the k shortest loopless paths in a network. Management Science 17, 712–716. doi:10.2307/2629312.

Zhang, Y., Shen, Z.J.M., Song, S., 2017. Lagrangian relaxation for the reliable shortest path problem with correlated link travel times. Transportation Research Part B: Methodological 104, 501–521. doi:10.1016/j.trb.2017.04.006.

Zockaie, A., Mahmassani, H.S., Nie, Y., 2016. Path finding in stochastic time varying networks with spatial and temporal correlations for heterogeneous travelers. Transportation Research Record: Journal of the Transportation Research Board 2567, 105–113. doi:10.3141/2567-12.

Zockaie, A., Nie, Y., Wu, X., Mahmassani, H., 2013. Impacts of correlations on reliable shortest path finding: A simulation-based study. Transportation Research Record: Journal of the Transportation Research Board 2334, 1–9. doi:10.3141/2334-01.

Zou, Y., Zhu, X., Zhang, Y., Zeng, X., 2014. A space–time diurnal method for short-term freeway travel time prediction. Transportation Research Part C: Emerging Technologies 43, 33–49. doi:10.1016/j.trc.2013.10.007.